# Study on Generalized Buffer-State-Based Relay Selection in Cooperative Cognitive Radio Networks

Master Thesis
修士論文

# Study on Generalized Buffer-State-Based Relay Selection in Cooperative Cognitive Radio Networks
# (協調コグニティブ無線におけるバッファ支援中継の選択手法に関する研究)

The University of Tokyo
Graduate School of Information Science and Technology
Department of Information and Communication Engineering

48-186407
張　睿超　　Ruichao ZHANG
Thesis Supervisor: 瀬崎　薫　Kaoru SEZAKI
Professor of Information and Communication Engineering

January 2020

## ABSTRACT

In the conventional relaying protocols, relays without buffers are considered. As a result, relay nodes are usually assigned to receive a packet from a source node in odd time slots, and forward it to a destination node in even time slots. However, such prefixed scheduling may impose significant degradation on system performance. For additional flexibility in the relay selection, the buffer-aided relay is considered as an effective technique to improve the performance gain. There are two classical buffer-aided relay selection schemes named the max-max and the max-link relay selection schemes. Based on these two schemes, many other relay selection schemes have been proposed in recent years. Also, the buffer-aided relay has been investigated in the context of the cognitive radio network.

In this thesis, we proposed a novel buffer-state-based relay selection scheme in the cooperative cognitive radio network, supporting the primary and secondary networks. In the proposed scheme, both the effects of inter-network interference and channel fading are successfully suppressed by introducing a flexible link selection algorithm in the secondary network. More specifically, by relying on the broadcast nature of wireless communication channels between a source node and relay nodes in the secondary network, the associated source packet is shared among multiple relay nodes. This allows us to benefit from the additional degree of freedom. Furthermore, we considered the priority for link selection, based on the buffer state of each secondary relay node. This contributes to the avoidance of detrimental empty and full buffer states. Moreover, analytical bounds of the outage probability and average packet delay were derived for the proposed scheme, based on the Markov chain model, which is verified by the numerical analyses of the proposed scheme. The diversity order, as well as the required overhead, was also investigated. Our numerical results demonstrated that the proposed scheme achieved better outage and packet-delay performance than the conventional max-ratio-based scheme in the buffer-aided cognitive radio network.

# Acknowledgements

First and foremost, I would like to show my deepest gratitude to my supervisor Prof. Kaoru Sezaki for his impressive kindness and enlightening instructions. His keen and vigorous academic observation was a milestone in the accomplishment of this thesis.

My appreciations also go to Prof. Shinya Sugiura and Dr. Ryota Nakai, who made my research successful and assisted me at every point during my research to achieve my goal. I also would like to thank all the lab mates at the Sezaki laboratory. Thanks a lot to Ms. Kaho Matsumoto and Ms. June Naito, who helped me deal with a lot of paperwork.

Finally, I would like to acknowledge with gratitude, the support of my family. They all kept me going, and this thesis would not have been possible without them.

January, 2020

# Contents

# Chapter 1

# Introduction

## 1.1 Background

Nowadays, wireless communication plays an increasingly significant role in our society. Many researchers tried to design a communication system with a faster transmission rate, in order to pursue higher system performance. However, Shannon has pointed out that the upper bound of the transmission rate is the channel capacity if reliable communication over a discrete memoryless channel is expected [1]. On the other hand, if the transmission rate is higher than the channel capacity, it is impossible to achieve reliable communication. The Shannon capacity with the additive white Gaussian noise channel can be expressed by $C = W \log_2(1 + \frac{\tilde{P}}{N_0 W})$, where $W$ is the bandwidth of the channel, $\tilde{P}$ is the received signal power, and $N_0$ is the noise power spectral density. For the performance evaluation, the Shannon capacity with $W = 1$ is usually considered, and so is this thesis. Different from the cable communication network, wireless communication is usually affected by the channel fading. If we denote the transmission power and channel coefficient as $P$ and $h$, respectively, the channel gain $\gamma = |h|^2$, and we have $\tilde{P} = P\gamma = P|h|^2$. Note that the channel gain $\gamma$ is directly associated with the channel capacity, and thus with the transmission rate. In order to mitigate the detrimental effects yielded by the channel fading, the cooperative communication was proposed [2, 3], which is one of the effective ways of improving the diversity gain in the spatial domain. Cooperative communication attains high diversity performance by using the fact that multiple independent transmission links have a low probability of experiencing deep fades simultaneously [4].

## 1.2 Cooperative Communication

As mentioned above, in the wireless communication system, the signal experiences various attenuations through the whole propagation process, which is known as the channel fading. For instance, due to the reflection and refraction by the water bodies and the terrestrial objects, the signal arrives at the receiving antenna through two or more paths with different delays, as Fig. 1.1 shows. This phenomenon is called the multipath propagation, which leads to the multipath fading. Multipath fading is usually characterized as the Rayleigh fading model since Rayleigh fading is viewed as a reasonable model for the environments such as the heavily built-up urban areas. Hence, all the transmission links

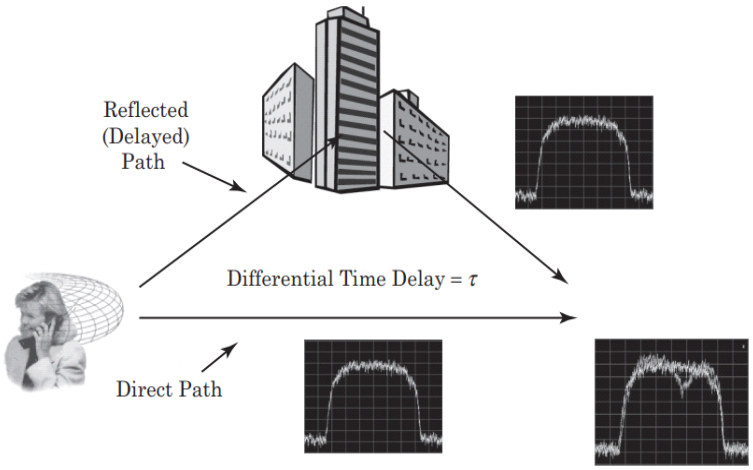


Figure 1.1: Multipath fading in wireless communication[1].

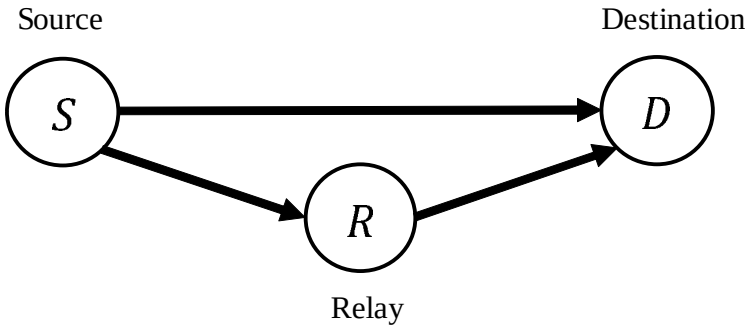


Figure 1.2: System model of three-terminal communication channel [6].

in the system models of this thesis are assumed to experience Rayleigh fading, where the channel gain is exponentially distributed.

To combat the multipath fading, relay technique is proposed. As one of the advantages, the relay technique is regarded as an effective way to mitigate fading effects by introducing spatial diversity [5], offering better quality of the communication link. Since there exists attenuation of the signal with distance, with the help of the relay technique, we can extend the coverage of the wireless communication system by dividing a single long-range link into several successive short-range links. Besides, system throughput can be efficiently increased with the relay technique.

Here, we introduce several basic system models of wireless communication and focus on the system model of the two-hop wireless communication with multiple relay nodes. Cooperative communications is a specific area of wireless communication that has been extensively explored within the last decade. As a significant method to enhance reliability and throughput in wireless systems, the cooperative communication system model was first proposed by van der Meulen [6]. In the system model shown in Fig 1.2, there

[1]source: https://m.eet.com/media/1116127/mcclaning_3_pt2.pdf

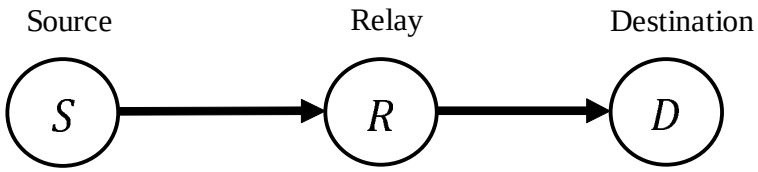


Figure 1.3: System model of two-hop wireless communication with a single relay node.

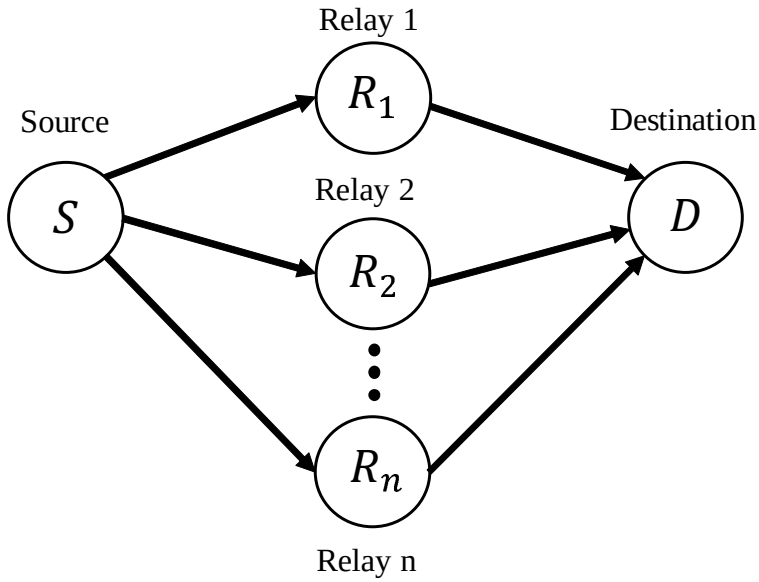


Figure 1.4: System model of two-hop wireless communication with multiple relay nodes.

are three nodes, namely, a source node, a relay node, and a destination node. The signal is transmitted in two phases. In phase I, the source node broadcasts its signal to the relay node and the destination node. Then, in phase II, the relay node forwards the received signal to the destination node, together with the transmission by the source node. The destination node combines the signals from the source and the relay node, in order to obtain the spatial diversity.

If the destination node can only receive the signal forwarded by the relay node, this kind of system model belongs to the multi-hop wireless communication, as shown in Fig. 1.3. It is used primarily to combat the signal attenuation in the long-range communication, since a single long-range link can be replaced with a chain of short-range links by placing several nodes between the source and the destination. Since the source node accomplishes the end-to-end communication with the aid of an intermediate relay node through the source-relay and the relay-destination links, system model in Fig. 1.3 is the two-hop communication. Studies on two-hop communication have shown that using multiple relay nodes, rather than a single one, can significantly improve the system throughput and reliability. This is mainly because the utilization of multiple relay nodes introduces more additional and independent links, thus improving the spatial diversity [7]. In this thesis, we focus on this system model shown in Fig. 1.4 and give

an overview of several relay selection schemes using conventional relays and buffer-aided relays in Chapter 2.

For cooperative communication, amplify-and-forward (AF) and decode-and-forward (DF) are two main relaying protocols. In the AF protocol, the relay node only amplifies the received signal and forwards the amplified signal, while in the DF protocol, the relay node first decodes the received signal and then forwards the re-encoded signal. Additionally, half-duplex (HD) and full-duplex (FD) are two main transmission modes of the relay node. In the HD mode, two orthogonal time or frequency channels are allocated for respective transmission and reception at the relay nodes, while the FD mode allows the simultaneous transmission and reception on the same frequency. Although the FD mode is capable of achieving double the channel capacity of the HD mode theoretically, the relay node suffers from a significant level of loop interference [8]. Throughout this thesis, half-duplex relay nodes using the DF protocol are considered.

## 1.3 Cognitive Radio Network (CRN)

With the rapid development of wireless communication, more and more spectrum resources are required to satisfy the different needs of various services. However, all the frequency bands are exclusively allocated to certain licensed users, and the spectrum sharing is not allowed. On the other hand, most of the licensed spectrum is under-utilized [9]. Due to the explosively growing demand for the bandwidth, it becomes urgent to enhance the spectrum efficiency. Hence, the cognitive radio network (CRN) was proposed [10], in order to deal with such problem. CRN allows the unlicensed users to access the licensed spectrum dynamically to enhance the frequency spectrum efficiency effectively, which is conducive to alleviating the current contradiction between the scarcity of radio spectrum resources and the rapid growth of users' requirements for wireless communications. However, CRN also has to face new challenges due to the fluctuating nature of the available spectrum, as well as the diverse quality of service requirements of various applications [11]. To address these challenges, several functions including the spectrum sensing, spectrum decision, spectrum sharing, and spectrum mobility [12].

The CRN mainly consists of a primary network (PN) and a secondary network (SN), where the primary user (PU) in the PN is the licensed user having the lisenced spectrum, while the secondary user (SU) in the SN borrows the spectrum from the licensed user. The CRN can be mainly divided into three modes, namely, the underlay, overlay and interleave CRN. In the underlay CRN, which is investigated throughout this thesis, the PU and the SU can simultaneously communicate with their corresponding destination node. As a result, the SU is required to transmit under certain power constraint, in order to avoid imposing the detrimental interference to the PU. In the overlay CRN, cooperation between the PU and SU is allowed, where the PU can communicate with its destination node with the help of the SU. In the interleave CRN, the SU is only allowed to access the licensed spectrum when it is not occupied by the PU. Therefore, spectrum sensing is crucial for this mode, which enables the SU to acquire information about the spectrum, such as its availability and parameters.

## 1.4 Motivation and Contributions

The conventional buffer-aided relay selection schemes proposed in the context of the CRN failed to take into consideration the empty and full buffer states, which bring about the negative effects on the system performance. Hence, the underlying idea is to avoid the detrimental buffer states, in order to maximize the number of available links. Besides, although the utilization of broadcast channels has been investigated in the conventional relaying network, this idea has been unexplored in the buffer-aided cooperative CRN. Against this background, the novel contributions of this paper are listed as follows.

1) We herein propose a novel relay selection scheme that incorporates the simultaneous activation of multiple links between the secondary source node and the secondary relay nodes. More specifically, multiple copies of a source packet in the secondary network are stored in multiple SR nodes, which contributes to the increase of the coding gain as well as the decrease of the end-to-end packet delay. Importantly, the proposed selection algorithm is designed to satisfy the requirement specific to the CRN.

2) Another contribution is that we introduce the concept of BSB relay selection into the proposed scheme. This allows us to avoid detrimental empty and full buffer states, thus maximizing the number of available links. Our numerical results demonstrate that the proposed scheme achieves better outage and packet-delay performance than the conventional max-ratio scheme [13]. Additionally, the effects of the asymmetric channels are also investigated, where the outage and packet-delay performance of the max-ratio scheme [13] and the proposed scheme are given.

3) Analytical bounds of the outage probability and average packet delay of the proposed scheme are derived based on the Markov chain model under the assumption of independent and identically distributed fading. This validates the system model and the numerical results of our scheme. Moreover, the theoretical diversity order is presented, which reveals the physical meaning of the proposed scheme. Finally, the overhead required for the secondary destination node of the proposed scheme is compared with that of the conventional scheme.

## 1.5 Outline of the Thesis

The remainder of this thesis is organized as follows. In Chapter 2, related works concerning the buffer-aided relay selection in the conventional network and the CRN are introduced. The comparison of the associated schemes, as well as their theoretical analyses, are presented. In Chapter 3, relay selection in the context of the CRN is analyzed. We present the system model of the buffer-aided cooperative CRN, and the generalized buffer-state-based relay selection is proposed here. The theoretical analysis and theoretical results of the proposed scheme are provided in Chapter 4. In this chapter, theoretical analysis of the outage probability and average packet delay are investigated. Besides, the diversity order and the required overhead are also discussed. Then, we provide the numerical results of the outage probability and average packet delay in Chapter 5, where

the study on the effects of the asymmetric channels is included. Finally, the thesis is concluded and future work is discussed in Chapter 6.

# Chapter 2

# Related Works

In this chapter, we first give an overview of the buffer-aided relaying protocols. Then, we focus on several relay selection schemes based on the two-hop multi-relay wireless communication model. The conventional relay selection scheme is introduced first, followed by the buffer-aided relay selection schemes in the conventional network. Finally, the application of the buffer-aided relay in the CRN is introduced. All the relay selection schemes herein considered the independent and identically distributed Rayleigh fading channels for all transmission links.

## 2.1 Preliminary Work

In wireless communications, relay selection has been exploited for introducing path diversity [14]. However, in the conventional relay selection schemes, the achievable performance is limited to the number of the relay nodes, due to the fixed schedule of transmission and reception [7]. In order to enhance the achievable diversity performance of the conventional relaying schemes, the buffer-aided cooperative relaying protocols have attracted much attention [15, 16, 17, 18, 19, 20, 21, 22, 23, 24]. Max-max relay selection (MMRS) [15] and max-link relay selection [17] schemes are two popular schemes developed for the two-hop buffer-aided cooperative network. As mentioned in [22], the MMRS scheme achieved a lower average packet delay than the max-link scheme, while the max-link scheme attained the maximum attainable diversity performance. In order to further improve the diversity order, Luo and Teh [20] introduced the concept of buffer-state-based (BSB) relay selection, where the qualified relay node is selected based on the buffer states of each relay node, in order to avoid detrimental empty and full buffer states.

Most of the buffer-aided relay selection schemes [15, 16, 17, 20] are designed for selecting only a single transmission link at each time slot. In order to introduce an additional design degree of freedom, the generalized MMRS (G-MMRS) and generalized max-link (G-ML) schemes were proposed [21], which allow the simultaneous exploitation of multiple source-to-relay links. These two schemes are capable of attaining a lower average packet delay than the original MMRS and max-link counterparts, owing to the beneficial effects of packet sharing among multiple relay nodes. Furthermore, the concept of BSB relay selection in [20] was then introduced into the beamforming-assisted G-ML scheme [23], the full-duplex scheme [25], and the secure relaying scheme [26]. Since one of the challenges in the buffer-aided relaying protocols is an increasing average

packet delay [7], a relay selection scheme in [27] achieved a significant reduction of the packet delay, compared to the max-link scheme [17] by introducing a priority on the relay selection criterion. The relay selection scheme based on the channel and buffer state information was proposed, for the sake of reducing the outage probability while achieving a high throughput [28]. Another relay selection scheme [29] reduced the packet delay of the MMRS scheme [15] by incorporating the diversity- and delay-aware relay selection policy.

In [13], the buffer-aided relay selection was introduced to CRN, which is referred to as the max-ratio scheme, where one out of all the available relay nodes in the secondary network is selected, so that the highest signal-to-interference ratio (SIR) is attained at the destination node of the secondary network. Furthermore, the concept of opportunistic interference cancellation is used for maximizing the throughput of the secondary network [30], while eliminating interference from the primary network to the secondary network. Also, in [31], the opportunistic cooperation scheme achieved a high throughput while maintaining a low delay, by introducing a priority into whether a user in the secondary network transmits its packet or support a user in the primary network to send a packet. Most recently, Kumar *et al.* incorporated adaptive link selection of [32] into the three-node two-hop buffer-aided CRN [33], where the trade-off between the packet delay, the system throughput, and the symbol error rate was investigated.

## 2.2 Conventional Relay Selection Schemes

In the cooperative communications, the half-duplex (HD) and full-duplex (FD) relaying protocols are two main relaying protocols, as mentioned in Section 1.2. However, many researchers focused on the HD relaying protocol, since it is difficult to implement the FD relaying protocols due to the strong self-interference. In the HD relaying protocol, the whole communication process from the source node to the destination node is divided into two time slots. As a result, a prefixed schedule of transmission and reception is considered in the conventional relaying schemes, where the source node transmits a packet to a relay node in odd time slots, and the corresponding relay node forwards the packet to the destination node in even time slots. However, such prefixed schedule may cause performance degradation, allowing for the time-varying nature of the wireless channels.

### 2.2.1 Best Relay Selection Scheme (BRS)

To elaborate further, we herein take as an example a well-known conventional relay selection scheme named best relay selection (BRS) scheme [**?**], which is considered as the optimal selection scheme for the conventional decode-and-forward relays without buffers.

#### System model

The system model of the BRS scheme consists of one source node, $S$, one destination node, $D$, and $K$ relay nodes $R_k$ ($k \in \{1, ..., K\}$). In this protocol, one relay node with the best end-to-end channel quality is chosen out of multiple available relay nodes, which

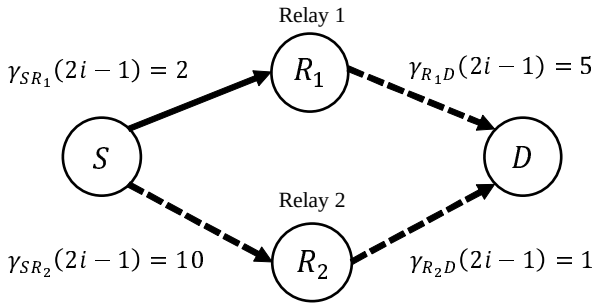


(a) In the time slot $(2i-1)$

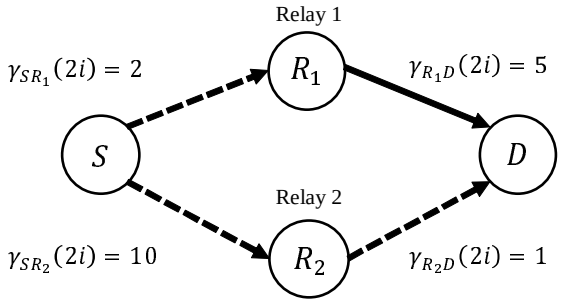


(b) In the time slot $2i$

Figure 2.1: An example of the BRS with $K=2$ relay nodes, where solid lines represent the link selected for packet transmission, while dashed lines represent the link not selected for packet transmission.

can be expressed by

$$R_b = \arg\max_{R_k \in \mathcal{C}} \{\min\{|h_{\text{S-R}_k}|^2, |h_{\text{R}_k\text{-D}}|^2\}\}, \tag{2.1}$$

where $h_{i-j}$ denotes the channel coefficient of the link from node $i$ to node $j$, and $\mathcal{C}$ is a cluster of all the relay nodes. Fig. 2.1 shows an example of the BRS scheme, where there exists two relay nodes in the system model, and $\gamma_{i-j} = |h_{i-j}|^2$ denotes the channel gain of the link from node $i$ to node $j$. We assume that all channels remain constant during every two successive time slots, and the source node transmits a packet to the selected relay node in odd time slots, while this relay node forwards the packet to the destination node in even time slots. Based on the BRS scheme, we first compare the channel gain of the S-R and R-D links for each relay node. From Fig. 2.1, we can know that

$$\min\{|h_{\text{S-R}_1}|^2, |h_{\text{R}_1\text{-D}}|^2\} = 2, \min\{|h_{\text{S-R}_2}|^2, |h_{\text{R}_2\text{-D}}|^2\} = 1. \tag{2.2}$$

Since the quality of the bottleneck link for the relay node $R_1$ (link S-$\text{R}_1$ here) is better than that for the relay node $R_2$ (link $R_2$-D here), $R_1$ is selected as the best relay in this case, according to the selection criterion of the BRS scheme. As an example in Fig. 2.1 shows, the packet is sent from the source node $S$ to the selected relay node $R_1$ in the odd time slot, and the relay node $R_1$ forwards the packet to the destination node $D$ in the even time slot. Since the relay nodes are not equipped with buffers, they must forward

the packet immediately to the destination node, whenever they receive the packet from the source node in the previous time slot. Hence, the transmission link from node $S$ to relay node $R_2$, which has the largest channel gain in Fig. 2.1, cannot be exploited. As a result, the prefixed schedule in the conventional relaying scheme prevents us from simultaneously exploiting the best available S-R and R-D links. To address this problem, relay selection schemes using the buffer-aided relays were proposed.

## 2.3 Buffer-aided Relay Selection Schemes

If the relay nodes are equipped with buffers, scheduling of the packet transmission and reception at the relay nodes will become more flexible, which allows more beneficial link selection during each packet transmission. Compared to the conventional schemes, buffer-aided relay selection schemes are able to significantly improve the system throughput, diversity and signal-to-noise ratio (SNR). However, some practical challenges, such as the overhead and the average packet delay, are also needed to be taken into consideration [32]. In this section, we introduce several buffer-aided relay selection schemes in the conventional network.

In the BRS scheme, it may be unable to simultaneously choose the best S-R and R-D links, as mentioned in Section 2.2. However, if relays are equipped with buffers, they can store the packets received from the source node and do not have to forward them immediately in the next time slot. This means that we can select the best relay nodes for transmission and reception, respectively. Such relay selection scheme is named as max-max relay selection (MMRS) scheme [15].

### 2.3.1 Max-max relay selection scheme (MMRS)

**System model**

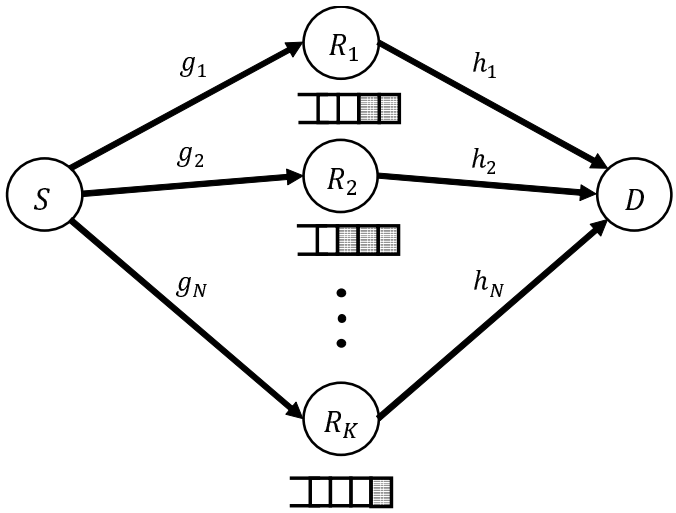


Figure 2.2: System model of the MMRS, where $g_k$ and $h_k$ ($k \in \{1, ..., K\}$) denote channel coefficients of the corresponding S-R and R-D links, respectively.

The system model of the MMRS scheme is shown in Fig. 2.2, which consists of one source node, $S$, one destination node, $D$, and $K$ half-duplex relay nodes $R_k$ ($k \in \{1, ..., K\}$) under the decode-and-forward mode. Time is considered to be slotted, and the transmission from the source node to the destination node spans over two time slots. It is assumed that the channel gain between the source node and the destination node is in deep fading. Thus, a direct link between these two nodes does not exist, and each relay node does not communicate with each other. Different from the system model of the BRS scheme, each relay node in the system model of the MMRS scheme is equipped with buffers. Moreover, the block fading model is considered here, where the channel coefficients are constant during the transmission of each packet, and vary independently from one packet to the next. Here, let $g_k$ and $h_k$ ($k \in \{1, ..., K\}$) denote the channel coefficient of the corresponding S-R and R-D links, respectively. Rayleigh fading channels are considered in [15] and hence, $g_k$ and $h_k$ are mutually independent zero-mean complex Gaussian random variables with variances $\sigma_{g_k}^2$ and $\sigma_{h_k}^2$, respectively. Then, let $\gamma_{g_k} = |g_k|^2 E_S/N_0$ and $\gamma_{h_k} = |h_k|^2 E_{R_k}/N_0$ denote the instantaneous SNR between the node $S$ and the node $R_k$, and that between the node $R_k$ and the node $D$, respectively. Here, $E_S$ is the transmission power of the node $S$, and $E_{R_k}$ is the transmission power of the node $R_k$. $N_0$ is the variance of the zero-mean additive white Gaussian noise (AWGN) at the node $R_k$ and the node $D$. Hence, $\gamma_{g_k}$ and $\gamma_{h_k}$ are exponentially distributed with parameters $1/\overline{\gamma}_{g_k}$ and $1/\overline{\gamma}_{h_k}$, respectively, where $\overline{\gamma}_{g_k} = \mathbb{E}[\gamma_{g_k}] = \sigma_{g_k}^2 E_S/N_0$, $\overline{\gamma}_{h_k} = \mathbb{E}[\gamma_{h_k}] = \sigma_{h_k}^2 E_{R_k}/N_0$, and $\mathbb{E}[\cdot]$ denotes the expectation.

In the MMRS scheme, since all the relay nodes are equipped with buffers, the best S-R and R-D links can be utilized. Hence, the best relay for packet reception is selected based on

$$R_{br} = \arg \max_{k \in \{1,...,K\}} \{\gamma_{g_k}\}, \tag{2.3}$$

and the best relay for transmission is selected based on

$$R_{bt} = \arg \max_{k \in \{1,...,K\}} \{\gamma_{h_k}\}. \tag{2.4}$$

The relay node selected for packet reception stores one packet transmitted from the source node in its buffer during the odd time slot. Under the assumption that each relay node forwards the packet in a first-come, first-served manner, this packet is then forwarded to the destination node until the associated relay node is selected for transmission, and all older packets in the queue of this relay node have been transmitted. During the even time slot, the relay node having the best R-D link is selected for transmission, and the first packet available in its buffer is forwarded.

Fig. 2.3 shows the case where the system has $K = 2$ relay nodes. In one odd time slot, since S-$R_2$ link is better than S-$R_1$ link, $R_2$ is selected as the best relay for receiving the source packet. Similarly, in the following even time slot, since $R_1$-D link is better than $R_2$-D link, $R_1$ is selected as the best relay for transmitting the packet to the destination node. Hence, due to the buffering capability at each relay node, the MMRS scheme is capable of utilizing the best S-R and R-D links at the same time. Obviously, all the relay nodes for packet reception should still have the empty space in their buffers, while should have at least one packet in their buffers for packet transmission. Hence, in the MMRS scheme, all the relay nodes are assumed to have infinite-sized buffers, in order

to make sure that the buffer of the selected relay node for packet reception is never full. Moreover, to ensure that the selected relay node for transmission always has a packet to send, a sufficiently large number of packets are sent from the source node to the destination node in an initialization phase before the system starts its normal operation.

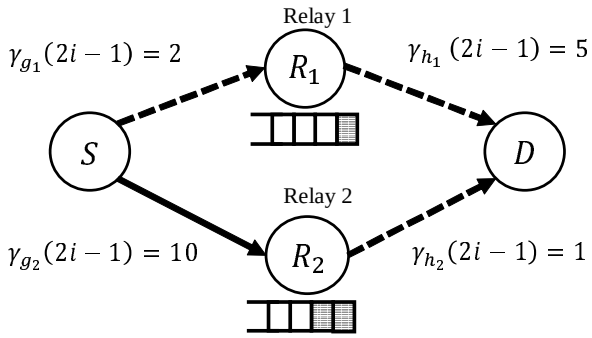


(a) In the time slot $(2i-1)$

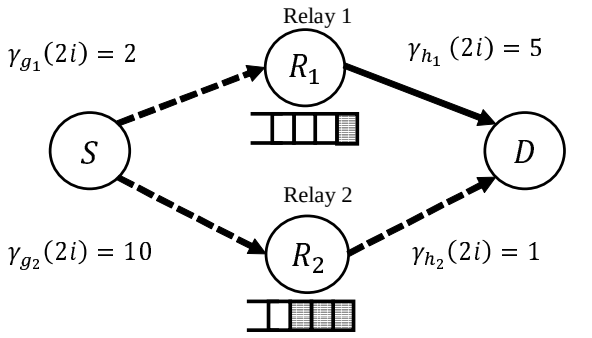


(b) In the time slot $2i$

Figure 2.3: An example of the MMRS scheme with $K=2$ relay nodes, where solid lines represent the link selected for packet transmission, while dashed lines represent the link not selected for packet transmission.

### Theoretical analysis

Here, the theoretical outage probability of the MMRS scheme is presented. The outage probability here is defined as the probability that the end-to-end channel capacity falls below the transmission rate. In the MMRS scheme, the channel capacity of the link between the node $S$ and the node $R_k$, and that between the node $R_k$ and the node $D$ are given by

$$C_{\text{S-R}_k} = \frac{1}{2}\log_2\left(1+\gamma_{g_k}\right), \tag{2.5}$$

$$C_{\text{R}_k\text{-D}} = \frac{1}{2}\log_2\left(1+\gamma_{h_k}\right), \tag{2.6}$$

respectively. For the MMRS scheme, if we let $\gamma_b = \min\{\gamma_{g_{b_r}}, \gamma_{h_{b_t}}\}$, where $\gamma_{g_{b_r}} = \max_{k\in\{1,...,K\}}\{\gamma_{g_k}\}$ and $\gamma_{h_{b_t}} = \max_{k\in\{1,...,K\}}\{\gamma_{h_k}\}$, the outage probability is given by

$$\begin{aligned} P_{\text{out}}^{MMRS} &= P(\min\{\gamma_{g_{b_r}}, \gamma_{h_{b_t}}\} \leq \gamma) \\ &= 1 - P(\gamma_{g_{b_r}} > \gamma)P(\gamma_{h_{b_t}} > \gamma) \\ &= 1 - [1 - P(\gamma_{g_{b_r}} \leq \gamma)][1 - P(\gamma_{h_{b_t}} \leq \gamma)] \\ &= 1 - [1 - \prod_{k=1}^{K}(1 - e^{-\frac{\gamma}{\overline{\gamma}_{g_k}}})][1 - \prod_{k=1}^{K}(1 - e^{-\frac{\gamma}{\overline{\gamma}_{h_k}}})], \end{aligned} \tag{2.7}$$

where $\gamma = 2^{2r_0} - 1$, and $r_0$ is the transmission rate. If we assume that the independent and identical distributed fading for both S-R and R-D links, namely, $\overline{\gamma} = \overline{\gamma}_{g_k} = \overline{\gamma}_{h_k}$, (2.8) can be simplified to

$$P_{\text{out}}^{MMRS} \approx (2^{\frac{1}{K}}\frac{\gamma}{\overline{\gamma}})^K. \tag{2.8}$$

### 2.3.2 Max-link relay selection scheme

The aforementioned relay selection schemes, both the BRS and the MMRS schemes, are associated with a two-slot protocol, where the packet transmission from the source node is fixed at odd time slots, and that from the relay node is fixed at even time slots. Thus, in order to relax this limitation and introduce more flexibility to the relay selection, the max-link relay selection scheme was proposed [17].

#### System model

The system model of the max-link relay selection scheme is a cooperative network, which consists of a source node $S$, a destination node $D$, and $K$ relay nodes, similar to the system model of the MMRS scheme, as shown in Fig. 2.2. In the MMRS scheme, the buffer size is assumed to be infinite, in order to ensure that the buffer of the relay node selected for packet reception is not full at any time. However, a more practical case where each relay node holds the finite-sized buffers is considered in the max-link relay selection scheme. More specifically, we assume that each relay node $R_k$ ($k \in \{1, ..., K\}$) is equipped with a data buffer $Q_k$ of finite size $L$, and let $\Psi(Q_k)$ denote the number of packets stored in the buffer of the relay node $R_k$. At the beginning of the transmission, the buffer of each relay node is empty. Here, the re-transmission process is based on an Acknowledgement / Negative-Acknowledgement (ACK / NACK) mechanism, where short-length error-free packets are broadcasted by the relay node or the destination node over a separate narrow-band channel, in order to inform the network of that packet's reception status.

All channels in the system model suffer from the frequency non-selective Rayleigh block fading, which means that the channel coefficient $h_{ij}$ remains constant during one time slot, but varies independently from one time slot to another, according to a circularly symmetric complex Gaussian distribution with zero mean and unit variance. Finally, the destination node is assumed to be able to have the perfect channel and buffer state information, which is used for selecting the relay nodes for transmission and

reception through an error-free feedback channel. Different from the MMRS scheme, the max-link relay selection scheme fully exploits the flexibility offered by the buffers at the relay nodes, and the strongest link is selected among all available links including the S-R and R-D links at each time slot. A S-R$_k$ link is considered to be available when $\Psi(Q_k) \neq L$, while $R_k$-D link is considered to be available when $\Psi(Q_k) \neq 0$. If a S-R link is the best link among all the available S-R and R-D links, the source node transmits a packet to the corresponding relay node, which means that $\Psi(Q_k)$ is increased by one when a packet is successfully decoded at the relay node $R_k$. On the other hand, if a R-D link is the strongest link, the corresponding relay node is selected for transmission, which means that $\Psi(Q_k)$ is decreased by one. Thus, the best relay for transmission or reception is selected based on

$$R_b = \arg\max_{R_k \in C} \{ \bigcup_{\Psi(Q_k)\neq L} \{|h_{\text{S-R}_k}|^2\}, \bigcup_{\Psi(Q_k)\neq 0} \{|h_{\text{R}_k\text{-D}}|^2\}\}, \tag{2.9}$$

where $h_{i-j}$ denotes the channel coefficient of the link from node $i$ to node $j$, and $C$ represents a cluster of all the relay nodes.

**Theoretical analysis**

For the max-link relay selection scheme, the outage probability is defined as the probability that the selected link is in an outage, which can be expressed by

$$P_{\text{out}} = \begin{cases} \Pr(\frac{1}{2}\log_2(1+P_t|h_{S-R_b}|^2) < r_0) & \textit{for relay reception} \\ \Pr(\frac{1}{2}\log_2(1+P_t|h_{R_b-D}|^2) < r_0) & \textit{for relay transmission}, \end{cases} \tag{2.10}$$

where $P_t$ is the transmission power of the source node and all the relay nodes, and $r_0$ is the transmission rate. Here, the variance of the AWGN is assumed to be normalized with zero mean and unit variance. Therefore, the SNR for each link is equal to $P_t$. Here, the Markov chain (MC) model, a general methodology to analyze the system having the relay nodes with finite-sized buffers, is introduced into the theoretical framework in order to deal with the outage probability analysis in [17]. Since a state of the MC denotes the number of elements in the buffers of each relay node here, let $s_l = (\Psi(Q_1)\Psi(Q_2)...\Psi(Q_K))$ denote the $l$-th state of the MC, where $1 \leq l \leq (L+1)^K$. Then, let $\mathbf{A} \in (L+1)^K \times (L+1)^K$ denote the state transition matrix of the MC, where $\mathbf{A}_{ij} = \Pr(s_j \to s_i) = \Pr(X_{t+1} = s_i | X_t = s_j)$ is the transition probability to move from state $s_j$ at time $t$ to state $s_i$ at time $(t+1)$. It is worth mentioning that the transition probability depends on the buffer state and the number of links that are not in an outage. More specifically, there is only one available S-R$_k$ link when $\Psi(Q_k) = 0$, since the relay node $R_k$ has no packet to send, and only one available R$_k$-D link when $\Psi(Q_k) = L$, since the buffer of the relay node $R_k$ has no additional space for another packet. Otherwise, the relay node $R_k$ offers two available links when $0 < \Psi(Q_k) < L$. In conclusion, the number of the available links that can be the candidates in the relay selection for state $s_l$ can be expressed by

$$D_l = \sum_{i=1}^{K} \Phi(Q_i), \tag{2.11}$$

where

$$\Phi(Q_i) = \begin{cases} 2 & for\ if\ 0 < \Phi(Q_i) < L \\ 1 & elsewhere. \end{cases} \tag{2.12}$$

For each time slot, changes of the buffer states can be categorized into three patterns: the number of the packets stored at one relay node (i) is decreased by one, if this relay node is selected for transmission; (ii) is increased by one, if this relay node is selected for packet reception, and the packet from the source node is decoded successfully; (iii) remains unchanged when an outage event happens, which means that the relay node $R_k$ is selected for packet reception, but the S-R$_k$ link is in an outage, or $R_k$ is selected for transmission, but the R$_k$-D link is in an outage. In order to formulate the above connectivity among the buffer states, let $U_l$ denotes the set that contains all the buffer states connected to state $s_l$ based on the above connectivity rule, which can be given by

$$U_l = \{ \bigcup_{1 \le i \le (L+1)^K} s_i : s_i - s_l \in \mathcal{Q}\}, \tag{2.13}$$

where $\mathcal{Q} = \{\bigcup_{1 \le j \le K} \pm \mathbf{I}_{j,\bullet}\}$. Here, $\mathbf{I}_{j,\bullet}$ denotes the $j$-th row of the identity matrix $\mathbf{I}$. Given the assumption for the independent and identically distributed links, the probability to select a specific link is equal to $1/D_l$ for state $s_l$, and the probability that this specific link is not in an outage can be calculated by using order statistics (the maximum among $D_l$ independent and identically distributed exponential random variables), hence the outage probability to leave from state $s_l$ can be expressed by

$$p_{D_l} = \frac{1}{D_l}[1 - (1 - e^{-\frac{2^{2r_0}-1}{P}})^{D_l}], \tag{2.14}$$

where $P$ is the transmission power of the source node and all the relay nodes. On the other hand, the outage probability for state $s_l$, which is the probability that there is no change in the buffer states, can be expressed by

$$\overline{p}_{D_l} = (1 - e^{-\frac{2^{2r_0}-1}{P}})^{D_l}. \tag{2.15}$$

Hence, the entries of the state transition matrix are given as

$$\mathbf{A}_{ij} = \begin{cases} \overline{p}_{D_l} & if\ s_i \notin U_j \\ p_{D_l} & if\ s_i \in U_j \\ 0 & elsewhere \end{cases}$$

$$\text{for } i, j \in \{1, \cdots, (L+1)^K\}. \tag{2.16}$$

It is proven that the state transition matrix $\mathbf{A}$ is irreducible and aperiodic, hence the stationary distribution vector $\boldsymbol{\pi} \in \mathbb{R}^{(L+1)^K}$ is given by

$$\boldsymbol{\pi} = (\mathbf{A} - \mathbf{I} + \mathbf{B})^{-1}\mathbf{b}, \tag{2.17}$$

where $\mathbf{B} \in \mathbb{R}^{(L+1)^K \times (L+1)^K}$ is a matrix with all elements to be one, and $\mathbf{b} = [1, \cdots, 1]^T \in \mathbb{R}^{(L+1)^K}$, while $\mathbf{I} \in \mathbb{R}^{(L+1)^K \times (L+1)^K}$ is the identity matrix. Thus, the outage probability of the system can be obtained as

$$P_{\text{out}} = \sum_{i=1}^{(L+1)^K} \boldsymbol{\pi}_i \overline{p}_{D_l} = \text{diag}(\mathbf{A})\boldsymbol{\pi}. \tag{2.18}$$

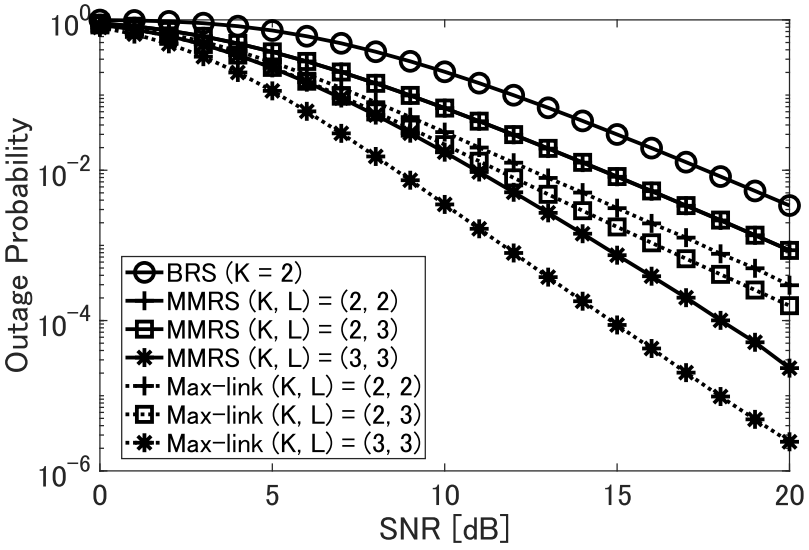


Figure 2.4: Outage probability of BRS, MMRS, and the max-link relay selection schemes, where the average SNR value was varied from 0 to 20 dB.

### 2.3.3 Other relay selection schemes

In the MMRS and the max-link relay selection schemes, only a single link is selected at each time slot. Hence, in order to introduce an additional degree of freedom, Oiwa et al., proposed the generalized MMRS (G-MMRS) and the generalized max-link (G-ML) relay selection schemes [21], which allow the simultaneous exploitation of S-R links. These two schemes are practical due to the broadcast nature of the wireless channels. As its explicit benefits, G-MMRS and G-ML schemes attained significantly lower average packet delay than the MMRS and max-link counterparts. However, the link selection in the G-MMRS and G-ML schemes are conducted without considering the buffer states of the relay nodes. Hence, the G-ML scheme was outperformed by the conventional max-link scheme in terms of the outage performance.

In order to address this problem, the generalized buffer-state-based scheme (GBSB) in the conventional network was proposed [23], which combines the concepts of simultaneous S-R link activations and BSB relay selection. Moreover, collaborative beamforming is also incorporated in [23], in order to improve the achievable performance. Since the most relay selection schemes consider the half-duplex relay in the system model, space full-duplex MMRS (SFD-MMRS) scheme was proposed [16], in order to avoid half-duplex loss. The SFD-MMRS scheme mimics the full-duplex relaying by allowing the simultaneous selection of different half-duplex relays for transmission and reception, so higher system throughput than that of the BRS and MMRS schemes is achieved. Studies on the buffer-aided relay technique combined with other techniques such as physical layer security are also significant research topics [24].

### 2.3.4 Numerical Results of BRS, MMRS and Max-link schemes

Here, the numerical results of the BRS, MMRS, and max-link relay selection schemes are presented. Throughout this section, the transmission rate $r_0$ is fixed to 1 bps/Hz, and $\sigma_{g_k}^2 = \sigma_{h_k}^2 = 1$, $E_S = E_{R_k}$ for the MMRS scheme, hence $\overline{\gamma} = \overline{\gamma}_{g_k} = \overline{\gamma}_{h_k} = \text{SNR}(k \in \{1, ..., K\})$. For the max-link scheme, $\text{SNR} = P_t$, as mentioned in Section 2.3.2.

Fig. 2.4 shows the outage probability of the above three schemes with different system parameters $(K, L)$, where BRS exhibited the worst outage performance, and the max-link scheme showed the best outage performance. When the number of the relay nodes increased, the outage performance improved in both the MMRS and the max-link schemes. Moreover, the outage performance of the max-link scheme increased when the buffer size became larger, while that of the MMRS scheme remained unchanged.

Note that it is assumed that the full or empty buffer state never appears in the MMRS scheme, as mentioned in Section 2.3.1, hence the outage performance of the MMRS scheme shown in Fig. 2.4 is under the idealistic assumption. This means that the outage performance of the MMRS scheme degrades when we consider a more practical system model, and the theoretical analysis presented in Section 2.3.1 is overestimated. However, the advantage of the MMRS scheme is that the update of the channel state information is once per two time slots, which is half of that of the max-link scheme [21].

## 2.4 Buffer-aided Relay Selection in the CRN

The cooperative communication has also been investigated in the context of the CRN. Similar to the relay selection schemes in the conventional network, research concerning the relaying protocols in the cooperative CRN also started with the relay nodes without buffers [34]. In [34], a max–min-based relay selection scheme extends the conventional BRS scheme into the CRN, where all the relay nodes are not equipped with buffers. In order to further improve the system performance and avoid the correlation problem among the available links as the selected candidates in [34], the max-ratio relay selection scheme was proposed [13].

### 2.4.1 Max-ratio Relay Selection Scheme

#### System model

The system model of the max-ratio relay selection scheme is shown in Figs. 2.5(a) and 2.5(b), where there is one primary source (PS) node, one primary destination (PD) node, one secondary source (SS) node, one secondary destination (SD) node, and $K$ secondary relay (SR) nodes. Since all the relay nodes work in the half-duplex mode, the whole communication process is divided into two phases, namely the SS-SR and the SR-SD transmission phases. In the former, the SS node transmits a packet to the selected SR node, while in the latter, the selected SR node forwards a packet to the SD node. Besides, each relay node is equipped with a data buffer $\Psi_k$ $(k \in \{1, ..., K\})$ of finite size $L$. In the secondary network, a single link having the highest signal-to-interference ratio out of all the available links is selected, when the buffer of the corresponding SR node is not full when the SS-SR link is selected, or not empty when the SR-SD link is selected.

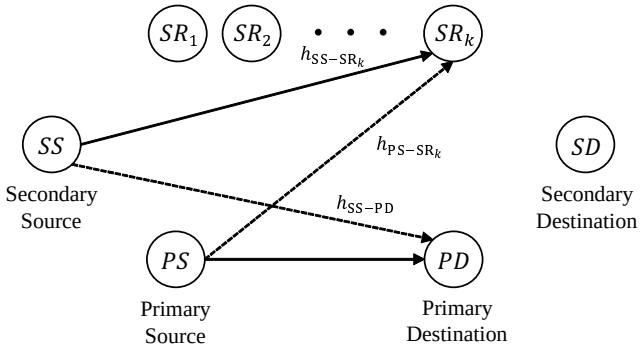


(a) SS-SR transmission

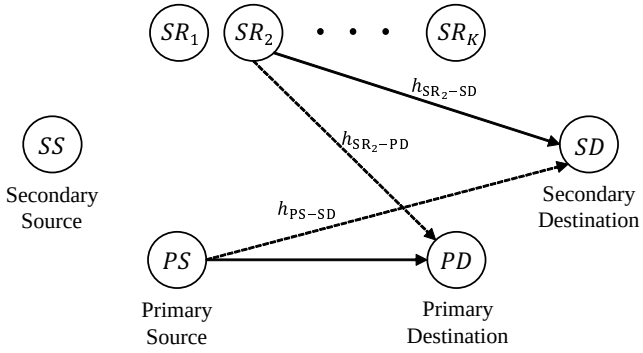


(b) SR-SD transmission

Figure 2.5: System model of the cooperative CRN, consisting of a one-hop primary and a two-hop secondary network: (a) SS-SR transmission and (b) SR-SD transmission.

Thus, the buffer-aided max-ratio relay selection policy is written by

$$R_{best,max-ratio} = \arg \max_{k\in\{1,2,\ldots,K\}} \{ \max_{\mathrm{SR}_k:\Psi_k\neq L} \{\mathrm{SIR}_{\mathrm{SR}_k}\}, \max_{\mathrm{SR}_k:\Psi_k\neq 0} \{\mathrm{SIR}_{\mathrm{SD}}\}\}. \tag{2.19}$$

where

$$\mathrm{SIR}_{\mathrm{SR}_k} = \frac{I_{\mathrm{th}}\gamma_{\text{SS-SR}_k}}{\gamma_{\text{SS-PD}}\gamma_{\text{PS-SR}_k}}, \tag{2.20}$$

$$\mathrm{SIR}_{\mathrm{SD}} = \frac{I_{\mathrm{th}}\gamma_{\mathrm{SR}_k\text{-SD}}}{\gamma_{\mathrm{SR}_k\text{-PD}}\gamma_{\text{PS-SD}}}. \tag{2.21}$$

Here, $\gamma_{a-b}$ denotes the channel gain of the transmission link from node $a$ to node $b$, and $I_{\mathrm{th}}$ denotes the predefined level, which is the maximum tolerable interference from the secondary network to the primary network. It is worth mentioning that the interference power from the primary network is dominant compared to the noise, hence the noise effects can be ignored at the receiving node at the secondary network [35].

**Theoretical analysis**

Here, the theoretical outage probability of the max-ratio scheme is presented, and the outage probability can be defined as

$$P_{\text{out}} = \begin{cases} \Pr(\frac{1}{2}\log_2(1+\text{SIR}_{\text{SR}_k}) < r_0) & for\ relay\ reception \\ \Pr(\frac{1}{2}\log_2(1+\text{SIR}_{\text{SD}}) < r_0) & for\ relay\ transmission, \end{cases} \tag{2.22}$$

where $r_0$ is the transmission rate. Since there exists $K$ relay nodes, and each relay node is equipped with a $L$-sized buffers, there are totally $(L+1)^K$ states. Here, the $l$-th state vector can be defined as $\text{s}_l = [\Psi_1^l, ..., \Psi_K^l]^{\text{T}}$ $l \in \{1, ..., (L+1)^K\}$, where $\Psi_k^l$ denotes the number of packets stored at the relay node $SR_k$ at state $s_l$. We assume that state $s_l$ corresponds to the pair of $(K_{1,l}, K_{2,l})$, where $K_{1,l}$ and $K_{2,l}$ are the numbers of available SS-SR and SR-SD links at state $s_l$, respectively. By considering all the possible available $K_{1,l}$ SS-SR links and $K_{2,l}$ SR-SD links, the outage probability of the overall system can be obtained as

$$P_{\text{out}} = \sum_{l=1}^{(L+1)^K} \pi_l \bar{p}_{s_l}^{(K_{1,l},K_{2,l})}, \tag{2.23}$$

where $\bar{p}_{s_l}^{(K_{1,l},K_{2,l})}$ and $\pi_l$ is the outage probability and the stationary probability at state $s_l$, resprctively. According to (2.20) and (2.21), we separate the common terms $\gamma_{\text{SS-PD}}$ and $\gamma_{\text{PS-SD}}$ in (2.22), and (2.22) can be rewritten as

$$R_{best,max-ratio} = \arg \max_{k\in\{1,2,...,K\}} \{ \frac{\max\limits_{\text{SR}_k:\Psi_k\neq L} \{\frac{I_{\text{th}}\gamma_{\text{SS-SR}_k}}{\gamma_{\text{PS-SR}_k}}\}}{\gamma_{\text{SS-PD}}}, \frac{\max\limits_{\text{SR}_k:\Psi_k\neq 0} \{\frac{I_{\text{th}}\gamma_{\text{SR}_k\text{-SD}}}{\gamma_{\text{SR}_k\text{-PD}}}\}}{\gamma_{\text{PS-SD}}} \} \tag{2.24}$$

Next, we let $w_k = (I_{\text{th}}\gamma_{\text{SS-SR}_k}/\gamma_{\text{PS-SR}_k})$, $w = \max\{w_k\}$, and $x = (w/\gamma_{\text{SS-PD}})$. Similarly, we let $v_k = (I_{\text{th}}\gamma_{\text{SR}_k\text{-SD}}/\gamma_{\text{SR}_k\text{-PD}})$, $v = \max\{v_k\}$, and $y = (v/\gamma_{\text{PS-SD}})$. Finally, we let $z = \max\{x, y\}$ to complete the max-ratio relay selection for the overall system. Based on the definition of the outage probability, if we denote the transmission rate by $r_0$, $\bar{p}_{s_l}^{(K_{1,l},K_{2,l})}$ can be further expressed by

$$\bar{p}_{s_l}^{(K_{1,l},K_{2,l})} = P(z < r_0) = F_Z(z = S_{th}), \tag{2.25}$$

where $F_Z(z)$ is the cumulative distribution function of $z$, and $S_{th} = 2^{2r_0} - 1$. Since $x$ and $y$ are independent, $F_Z(z) = F_X(z)F_Y(z)$. The closed-form of $F_X(x)$ can be obtained as

$$F_X(x) = \begin{cases} 1 & if\ K_{1,l} = 0, \\ 1 - \frac{L_1}{\lambda_{\text{SS-PD}}x} e^{\frac{L_1}{\lambda_{\text{SS-PD}}x}} \text{Ei}(1, \frac{L_1}{\lambda_{\text{SS-PD}}x}) & if\ K_{1,l} = 1, \\ (\frac{\lambda_{\text{SS-PD}}x}{L_1})^{K_{1,l}-1} \frac{\mathcal{MG}([[0],[]],[[K_{1,l}-1,K_{1,l}],[]],\frac{L_1}{\lambda_{\text{SS-PD}}x})}{\Gamma(K_{1,l})} & elsewhere, \end{cases}$$

where $\text{Ei}(1, a) = \int_1^\infty (e^{-at}/t)dt (a > 0)$, $\Gamma(\cdot)$ is the gamma function, and $\mathcal{MG}([[], []], [[\cdot, \cdot], []], \cdot)$ is the Meiher G function [36]. On the other hand, $F_Y(y)$ can be similarly obtained as (2.26).

Here, the independent and identically distributed fading is considered, hence the probability to select any transmission link is equable as $1/(K_{1,l} + K_{2,l})$ at state $s_l$.

Hence, if we denote $U_l$ as the set containing all the states that can be moved from state $s_l$ through a one-step transition, the probability that state $s_l$ moves to a state in $U_l$ is given by

$$p_{s_l} = \frac{1 - \bar{p}_{s_l}^{(K_{1,l},K_{2,l})}}{K_{1,l} + K_{2,l}}. \tag{2.26}$$

We here denote $\mathbf{A}$ as the state transition matric, where $\mathbf{A}_{n,l} = P(X_{t+1} = s_n | X_t = s_l)$. Here, $\mathbf{A}_{n,l}$ is the probability to move from state $s_l$ at time $t$ to state $s_n$ at time $(t+1)$. Then, we have

$$\mathbf{A}_{n,l} = \begin{cases} \bar{p}_{s_l}^{(K_{1,l},K_{2,l})} & if\ s_n = s_l, \\ p_{s_l} & if\ s_n \in U_l, \\ 0 & elsewhere. \end{cases}$$

Since the transition matrix $\mathbf{A}$ is column stochastic, irreducible, and aperiodic [17], the stationary distribution vector is obtained as

$$\boldsymbol{\pi} = (\mathbf{A} - \mathbf{I} + \mathbf{B})^{-1}\mathbf{b}, \tag{2.27}$$

where $\mathbf{B} \in \mathbb{R}^{N_{\text{state}} \times N_{\text{state}}}$ is a matrix with all elements to be one, and $\mathbf{b} = [1, \cdots, 1]^T \in \mathbb{R}^{N_{\text{state}}}$, while $\mathbf{I} \in \mathbb{R}^{N_{\text{state}} \times N_{\text{state}}}$ is the identity matrix. Thus, the outage probability of the whole system can be obtained as [17]

$$P_{\text{out}} = \text{diag}(\mathbf{A})\boldsymbol{\pi}. \tag{2.28}$$

## 2.5 Summary

In this chapter, the related works concerning the buffer-aided relay selection schemes are introduced. Both the numerical and theoretical analysis are presented, which is the foundation of this thesis. Especially, the max-link and the max-ratio relay selection schemes select the best link among $2K$ available links, under the assumption that all the relay nodes are equipped with infinite-sized buffers, where $K$ is the number of the relay nodes. As a result, the diversity order approaches $2K$ if the buffer of each relay node is large enough. However, for the relay nodes with finite-sized buffers, which is a more practical case, the number of the available links is less than $2K$. Besides, the correlation problem in the CRN also constraints the max-ratio scheme from attaining the full diversity order.

# Chapter 3

# Generalized Buffer-State-Based Relay Selection in the CRN

In this chapter, the proposed buffer-state-based relay selection scheme is presented in the context of the cooperative CRN. The system model of the proposed scheme, as well as the priority classification and the decision algorithm for link activation, is elaborated. Specifically, the process of secondary transmission in the proposed scheme consists of the broadcasting phase and the relaying phase, both of which are continuously affected by the primary network. We evaluated the priority of each link based on the buffer states of the corresponding SR nodes and proposed the decision algorithm to determine which link needs to be activated.

## 3.1 System Model

Figs. 3.1(a) and 3.1(b) show the broadcasting and the relaying phases of the proposed scheme, which amalgamates the concept of the BSB relay selection and the simultaneous activation of multiple SS-SR links, whose algorithms are shown in Tables 3.1 and 3.2, respectively.

As shown in Figs. 3.1(a) and 3.1(b), the cooperative CRN considered in this thesis is composed of the primary network (PN) and the secondary network (SN), and the underlay CRN is investigated throughout this paper. In the PN, a single primary source (PS) node maintains to directly communicate with a single primary destination (PD) node. The SN is a two-hop relaying one, consisting of a single secondary source (SS) node, a single secondary destination (SD) node, and $K$ secondary relay (SR) nodes. Here, the SS node communicates with the SD node via the SR nodes, assuming that no direct link exists between the SS and the SD nodes.

Additionally, all the SR nodes operate in the half-duplex mode under the decode-and-forward principle. This implies that the packet transmission from the SS node to the SD node spans over two time slots. Note that the SR nodes are introduced for improving the communication quality of the secondary user, since the transmission power of the SN is contaminated due to interference from the PN. In this thesis, we focused our attention on the performance of the SN, and hence we assume the assistance of the relay nodes only in the SN, for simplicity. The channel coefficient and the channel gain between arbitrary two nodes, i.e., a node $a$ and a node $b$, are represented by $h_{a\text{-}b}$ and $\gamma_{a\text{-}b} = |h_{a\text{-}b}|^2$, respectively. Furthermore, the corresponding average channel gain is

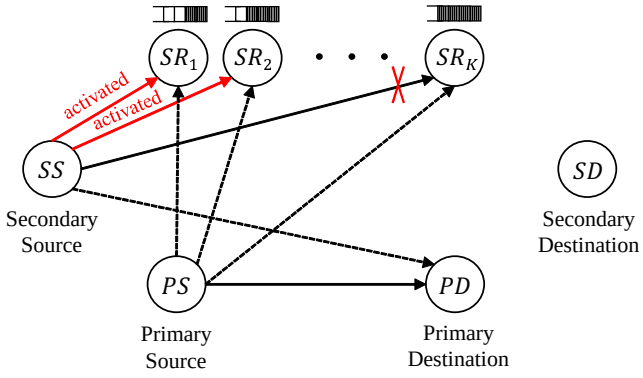


(a) Broadcasting Phase

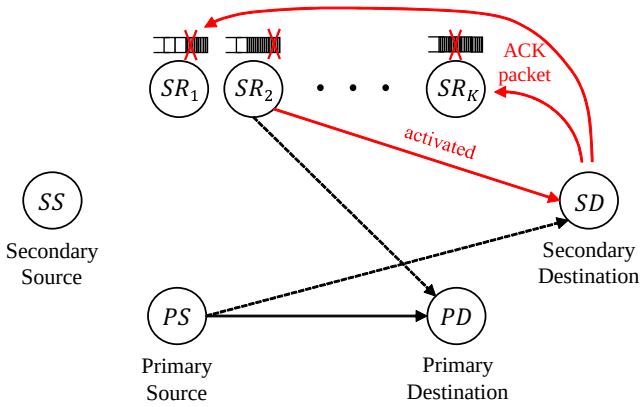


(b) Relaying Phase

Figure 3.1: System model of the proposed scheme, which simultaneously activates multiple links in the broadcasting phase: (a) broadcasting phase and (b) relaying phase.

represented by $\mathbb{E}[\gamma_{a\text{-}b}] = \lambda_{a\text{-}b}$. Unless otherwise noted, in this thesis we mainly consider the independent and identically distributed Rayleigh fading channels for all the SS-SR and SR-SD links, where $\lambda_{\text{SS-SR}_k} = \lambda_{\text{SR}_k\text{-SD}}$ ($k \in \{1, ..., K\}$). The $k$-th SR node, i.e., the $\text{SR}_k$ node ($k \in \{1, 2, \cdots, K\}$), has a data buffer of finite size $L$, and the number of the packets stored at the $\text{SR}_k$ node is represented by $\Psi_k$ ($0 \leq \Psi_k \leq L$). Note that $\Psi_k$ is increased by one if the $\text{SR}_k$ node successfully decodes a packet transmitted from the SS node. Similarly, $\Psi_k$ is decreased by one if the SD node successfully receives and decodes a packet transmitted from the $\text{SR}_k$ node. Moreover, the $\text{SR}_k$ node transmits its queued packets to the SD node in a first-come, first-served manner.

Throughout this thesis, we focus our attention on the scenario of a fixed transmission rate of $r_0$ [bps/Hz], rather than that of an adaptive transmission rate. All the channel coefficients are assumed to be independent Rayleigh fading, which are generated as mutually independent random variables, obeying the zero-mean complex-valued Gaussian distribution. Moreover, we assume that each channel coefficient remains constant during a single time slot. Furthermore, the SD node acts as a central coordinator, which periodically collects all the channel coefficients, as well as the buffer states, and transmits

control packets to the SR nodes, similar to the previous studies[15, 17, 18, 21, 22]. If the channel capacity of a specific link is higher than the transmission rate of $r_0$, the packet can be successfully decoded at the receiving node. Additionally, we assume that there are stable low-rate feedback channels, where an acknowledge (ACK) packet is sent from the SD node to all the SR nodes if the SD node successfully decodes the packet. Note that this is the same assumption as that considered in [21, 22, 23, 26]. Since we assume that the SD node periodically transmits control packets to the SR nodes, the ACK packet can also be sent in a piggy-back manner. Hence, the required overhead and the related interference may be maintained to be minimum [23]. When the SR nodes receive the ACK packet, multiple copies of the associated packet stored in the buffers are deleted.

Similar to [13], in the PN, the PS node continues to transmit its source packets to the PD node. In the SN, either the SS node or the SR node tries to transmit or relay its source packet. Due to the presence of the interference from the PS node to the SR and SD nodes, the signals received at the $\mathrm{SR}_k$ node selected for packet reception are given by

$$y_{\mathrm{SR}_k} = \sqrt{P_{\mathrm{SS}}} h_{\text{SS-SR}_k} x_{\mathrm{SS}} + \sqrt{P_{\mathrm{PS}}} h_{\text{PS-SR}_k} x_{\mathrm{PS}} + n_{\mathrm{SR}_k}, \tag{3.1}$$

where $x_{\mathrm{SS}}$ and $x_{\mathrm{PS}}$ denote the source signals transmitted from the SS and the PS nodes, respectively. Furthermore, $P_{\mathrm{SS}}$ and $P_{\mathrm{PS}}$ are the transmission powers of the SS and PS nodes, respectively. Also, $n_{\mathrm{SR}_k}$ represents the additive white Gaussian noise (AWGN) at the $\mathrm{SR}_k$ node. Similarly, in the SR-SD transmission phase, where the packet is forwarded from the selected SR node to the SD node, the signals received at the SD node are given by

$$y_{\mathrm{R}_k\mathrm{D}} = \sqrt{P_{\mathrm{SR}_k}} h_{\text{SR}_k\text{-SD}} x_{\mathrm{SR}_k} + \sqrt{P_{\mathrm{PS}}} h_{\text{PS-SD}} x_{\mathrm{PS}} + n_{\mathrm{SD}}, \tag{3.2}$$

where $x_{\mathrm{SR}_k}$ denotes the symbol relayed from the $\mathrm{SR}_k$ node, and $P_{\mathrm{SR}_k}$ denotes the transmission power of the $\mathrm{SR}_k$ node. Also, $n_{\mathrm{SD}}$ represents the AWGN at the SD node. In order to guarantee the communication quality of the PN, the packet transmission of the SN is allowed only when its interference power to the PN is below a predefined level. Since the interference power from the SS node and the $\mathrm{SR}_k$ node to the PN is given by $P_{\mathrm{SS}}\gamma_{\text{SS-PD}}$ and $P_{\mathrm{SR}_k}\gamma_{\text{SR}_k\text{-PD}}$, respectively, if we let $I_{\mathrm{th}}$ denote the predefined level, the SN has to satisfy the power constraints of $P_{\mathrm{SS}}\gamma_{\text{SS-PD}} \leq I_{\mathrm{th}}$ and $P_{\mathrm{SR}_k}\gamma_{\text{SR}_k\text{-PD}} \leq I_{\mathrm{th}}$. Here, we assume that the SS and the SR nodes can obtain the CSI of SS-PD and SR-PD links, respectively, so that the SS and the SR nodes can adjust their transmission power accordingly. More specifically, the PD node is considered to periodically broadcast a pilot block to the SS node and all the SR nodes. Then, the SS node and the $\mathrm{SR}_k$ node carry out the CSI estimation of the PD-SS and PD-$\mathrm{SR}_k$ links, respectively, based on the received pilot block. For simplicity, we assume that the time-division duplexing is used here [37], where the CSI of the SS-PD and SR-PD links can be estimated on the basis of the CSI estimation of PD-SS and PD-SR links. The detailed implementations are out of the scope of this thesis, which are left for future studies. Without the loss of generality, the transmission power of the PS node $P_{\mathrm{PS}}$ is normalized to unity in this thesis. Hence, the signal-to-noise ratios at the $\mathrm{SR}_k$ node and the SD node are given by

$$\mathrm{SIR}_{\mathrm{SR}_k} = \frac{P_{\mathrm{SS}}\gamma_{\text{SS-SR}_k}}{P_{\mathrm{PS}}\gamma_{\text{PS-SR}_k}} = \frac{I_{\mathrm{th}}\gamma_{\text{SS-SR}_k}}{\gamma_{\text{SS-PD}}\gamma_{\text{PS-SR}_k}}, \tag{3.3}$$

$$\mathrm{SIR}_{\mathrm{SD}} = \frac{P_{\mathrm{SR}_k}\gamma_{\mathrm{SR}_k\text{-SD}}}{P_{\mathrm{PS}}\gamma_{\text{PS-SD}}} = \frac{I_{\mathrm{th}}\gamma_{\mathrm{SR}_k\text{-SD}}}{\gamma_{\mathrm{SR}_k\text{-PD}}\gamma_{\text{PS-SD}}}, \tag{3.4}$$

respectively, and the channel capacity of the link between the SS and $\mathrm{SR}_k$ nodes, and that between the $\mathrm{SR}_k$ and SD nodes are given by

$$C_{\text{SS-SR}_k} = \frac{1}{2}\log_2\left(1+\mathrm{SIR}_{\mathrm{SR}_k}\right), \tag{3.5}$$

$$C_{\mathrm{SR}_k\text{-SD}} = \frac{1}{2}\log_2\left(1+\mathrm{SIR}_{\mathrm{SD}}\right), \tag{3.6}$$

respectively. Since we assume that all the SR nodes operate in the half-duplex mode, a prelog factor of 1/2 is imposed on (3.5) and (3.6). Moreover, similar to the previous studies [13, 35], we ignore the effects caused by the AWGN when calculating the signal-to-noise ratios at the SR and SD nodes, by assuming that the interference from the PS node is dominant in comparison to the AWGN.

## 3.2 Proposed BSB Relay Selection Scheme

Table 3.1: Priority Classification of Available Links ($L \geq 3$)

| Priority | Low | High | Highest |
|---|---|---|---|
| SS-SR links | $\Psi_k = L-1$ | $\xi_{\text{SS-SR}} < \Psi_k < L-1$ | $0 \leq \Psi_k \leq \xi_{\text{SS-SR}}$ |
| SR-SD links | $\Psi_k = 1$ | $1 < \Psi_k < \xi_{\text{SR-SD}}$ | $\xi_{\text{SR-SD}} \leq \Psi_k \leq L$ |

Table 3.2: Decision Algorithm for Link Activation ($L \geq 3$)

| | $N_{\text{SS-SR}}^{Low}$ | $N_{\text{SS-SR}}^{High}$ | $N_{\text{SS-SR}}^{Highest}$ | $N_{\text{SR-SD}}^{Low}$ | $N_{\text{SR-SD}}^{High}$ | $N_{\text{SR-SD}}^{Highest}$ | Decision |
|---|---|---|---|---|---|---|---|
| Case1 | – | – | $\geq 1$ | – | – | – | Activate $N_{\text{SS-SR}}^{Highest} + N_{\text{SS-SR}}^{High}$ highest- and high-priority SS-SR links |
| Case2 | – | – | 0 | – | – | $\geq 1$ | Activate the single SR-SD link with the highest $\mathrm{SIR}_{\mathrm{SD}}$ out of $N_{\text{SR-SD}}^{Highest}$ highest-priority SR-SD links |
| Case3 | – | $\geq 1$ | 0 | – | – | 0 | Activate $N_{\text{SS-SR}}^{High}$ high-priority SS-SR links |
| Case4 | – | 0 | 0 | – | $\geq 1$ | 0 | Activate the single SR-SD link with the highest $\mathrm{SIR}_{\mathrm{SD}}$ out of $N_{\text{SR-SD}}^{High}$ high-priority SR-SD links |
| Case5 | – | 0 | 0 | $\geq 1$ | 0 | 0 | Activate the single SR-SD link with the highest $\mathrm{SIR}_{\mathrm{SD}}$ out of $N_{\text{SR-SD}}^{Low}$ low-priority SR-SD links |
| Case6 | $\geq 1$ | 0 | 0 | 0 | 0 | 0 | Activate the single SS-SR link with the highest $\mathrm{SIR}_{\mathrm{SR}_k}$ out of $N_{\text{SS-SR}}^{Low}$ low-priority SS-SR links |
| Case7 | 0 | 0 | 0 | 0 | 0 | 0 | No link activated (outage event) |

In order to avoid empty and full buffer states at the SR nodes, which is not considered in [13], we introduced the link priority used for BSB link selection. Here, we denote the number of SS-SR links and SR-SD links that are not in an outage as $N_{\text{SS-SR}}$ and $N_{\text{SR-SD}}$, respectively ($0 \leq N_{\text{SS-SR}}, N_{\text{SR-SD}} \leq K$). Once the SD node collects the buffer states of

the SR nodes, the SD node evaluates the priorities of all the available links, based on the classification criterion of Table 3.1. In this criterion, we introduced two additional thresholding parameters, i.e., $\xi_{\text{SS-SR}}$ and $\xi_{\text{SR-SD}}$, which are determined in advance of link selection.[2] The values of $\xi_{\text{SS-SR}}$ and $\xi_{\text{SR-SD}}$ are typically set to be low, in order to maintain a low average packet delay. Hence in this thesis, we set $(\xi_{\text{SS-SR}}, \xi_{\text{SR-SD}}) = (0, 2)$ for $L = 2$ and $(\xi_{\text{SS-SR}}, \xi_{\text{SR-SD}}) = (1, 2)$ for $L \geq 3$.

The $N_{\text{SS-SR}}$ available links between the SS and the SR nodes are classified into three groups with the low, high and highest priorities. When the number of the packets stored in the buffer of the $\text{SR}_k$ node is $\Psi_k = L-1$, the priority of the corresponding SS-SR link is set to low. Furthermore, the priority is set to high and highest when the number of the packets stored in the buffer is $\xi_{\text{SS-SR}} < \Psi_k < L-1$ and $0 \leq \Psi_k \leq \xi_{\text{SS-SR}}$, respectively. We denote the number of low-, high- and highest-priority links as $N^{Low}_{\text{SS-SR}}, N^{High}_{\text{SS-SR}}, N^{Highest}_{\text{SS-SR}}$, respectively, and have the relationship of $N_{\text{SS-SR}} = N^{Low}_{\text{SS-SR}} + N^{High}_{\text{SS-SR}} + N^{Highest}_{\text{SS-SR}}$. Similarly, the available $N_{\text{SR-SD}}$ links between the SR nodes and the SD node are also categorized into three groups with low, high and highest priorities, where the number of the links in each group is denoted by $N^{Low}_{\text{SR-SD}}, N^{High}_{\text{SR-SD}}, N^{Highest}_{\text{SR-SD}}$, respectively. However, unlike the broadcasting phase, when the number of the packets stored at the buffer of the $\text{SR}_k$ node is $\Psi_k = 1$, the priority of the associated SR-SD link is low. The priority is high and highest for $1 < \Psi_k < \xi_{\text{SR-SD}}$ and $\xi_{\text{SR-SD}} \leq \Psi_k \leq L$, respectively. Note that when the number of the packets stored at the SR node is close to the buffer size, the priority of the associated SS-SR link is low. This is for the sake of avoiding the full buffer state, which reduces the number of available links for link activation. Similarly, in the relaying phase, the low-priority link is such that the number of the packets stored at the corresponding SR node is one, in order to avoid the empty buffer state, which also reduces the number of the available links. Hence, the introduction of $\xi_{\text{SS-SR}}$ and $\xi_{\text{SR-SD}}$ in Table 3.1 contributes to the reduction of the potential empty and full buffer states, respectively.

After the decision of the priorities of all the available links, the SD node activates a single SS-SR link, multiple SS-SR links, or a single SR-SD link based on the decision algorithm for link activation, shown in Table 3.2, which lists all the cases from Case 1 to Case 7. When there is at least one SS-SR link with the highest priority, the $N^{Highest}_{\text{SS-SR}} + N^{High}_{\text{SS-SR}}$ highest- and high-priority SS-SR links are all activated in the broadcasting phase, which corresponds to Case1. As for Case 2, where there is no highest-priority SS-SR link, but there is at least one highest-priority SR-SD link, a single SR-SD link with the highest SIR at the SD node is activated among the $N^{Highest}_{\text{SR-SD}}$ SR-SD links. Moreover, in Case 3, where there is not any highest-priority SS-SR or SR-SD links, while at least one high-priority SS-SR link exists, the $N^{High}_{\text{SS-SR}}$ high-priority SS-SR links are all activated. Similar to Case 1, all the associated SR nodes simultaneously receive a source packet. When there is no highest- or high-priority SS-SR link, a single SR-SD link is activated, where high-priority one is activated in Case 4 and low-priority one is activated in Case 5. In Case 6, where there is no available link other than the low-priority SS-SR links, only a single SS-SR link having the highest SIR at the corresponding SR node is activated, in order to maximize the number of the available links. Finally, Case 7 corresponds to

[2]The effects of these two thresholding parameters on the outage probability and average packet delay are investigated later in Section 5.1, where the guidance of designing the values of $\xi_{\text{SS-SR}}$ and $\xi_{\text{SR-SD}}$ is provided.

an outage event, where there is neither an available SS-SR link nor an available SR-SD link. As mentioned in Section 3.1, when an SR-SD link is selected, an ACK packet is sent to all the SR nodes through stable low-rate feedback channels, after the SD node successfully decodes the packet. Then, multiple copies of the associated packet stored at the SR nodes are deleted from the buffers. The specific implementation is out of the scope of this paper, and the detailed investigations are left for future studies.

## 3.3 Summary

The novel relay selection scheme was proposed for the cooperative buffer-aided CRN in this chapter, which introduces two concepts including the simultaneous activation of multiple SS-SR links and buffer-state-based link selection. In order to make the best use of the broadcast nature of wireless communication channels, the proposed scheme incorporated the broadcasting phase, where the source packets of the secondary source node are shared among multiple qualified secondary relay nodes. Besides, motivated by several buffer-state-based relaying schemes in the conventional network, we imposed the priority for link selection based on the buffer states of each relay node, which contributes to avoiding the empty and full buffer states.

# Chapter 4

# Theoretical Analysis of GBSB Relay Selection

In this section, the theoretical bounds of the outage probability and average packet delay of the proposed scheme are derived based on the Markov chain model, which is suitable for the analysis of the system having the relay nodes with finite-sized buffers. Also, the diversity order, as well as the overhead required for the SD node of the proposed scheme, is presented. Since the purpose of the proposed scheme is to mitigate the multipath and fading effects, the outage probability is an appropriate metric for the performance evaluation [17], and this metric is also used in the related work [15, 16, 17, 18, 20, 21, 22, 23]. Besides, one of the challenges that the buffer-aided relaying is faced with is the increased average packet delay [7], hence this is another important evaluation metric for all buffer-aided relaying protocols. According to [21], the buffer-aided cooperative communications attain a high diversity gain at the cost of imposing the additional overhead, so it is meaningful to analysis the overhead required for monitoring CSI and buffer states in the CRN. [3] Similar to the conventional theoretical analysis [17, 22, 23], we assume that a sufficiently large number of packets are transmitted from the SS node to the SD node. For simplicity, we focused our attention on the specific scenario of $K = 2$ SR nodes with $(L = 2)$-sized buffers. However, the bounds derived in this chapter are readily applicable to arbitrary $(K, L)$ parameters.

## 4.1 State Transition Diagram

Table 4.1 lists all the legitimate buffer states of the SR nodes in the proposed scheme, where we have $N_{\text{state}} = 13$ states in total when $(K, L) = (2, 2)$, and four different symbols of $\bigcirc$, $\triangle$, $\square$, and $\diamond$ denote four different packets. In the proposed scheme, multiple SR nodes are allowed to share the same packet when the priorities of their corresponding SS-SR links are highest or high. Hence, in the four states of $s_{10}$, $s_{11}$, $s_{12}$, and $s_{13}$, multiple copies of the source packet are shared among $K = 2$ SR nodes.

Fig. 4.1 shows the state transition diagram of the Markov chain model of the proposed scheme. In order to clarify the state transition of Fig. 4.1, let us exemplify the transition

[3] Since we herein focused our attention on the performance evaluations of the secondary network in the underlay cognitive networks, the packet loss of the primary network was not investigated. Note that in the underlay cognitive radio network considered, the primary user and the secondary user simultaneously transmit packets, as long as the transmission power of the secondary user satisfies a power constraint. Hence, the probability of primary user detection, which is a typical parameter in the interleave cognitive radio network, is not chosen for analysis.

Table 4.1: Legitimate Buffer States of $K = 2$ Relay Nodes with $(L = 2)$-Sized Buffers

| States | Relay 1 | | Relay 2 | |
|---|---|---|---|---|
| $s_1$ | empty | empty | empty | empty |
| $s_2$ | ◯ | empty | empty | empty |
| $s_3$ | empty | empty | ◯ | empty |
| $s_4$ | ◯ | □ | empty | empty |
| $s_5$ | ◯ | empty | □ | empty |
| $s_6$ | empty | empty | ◯ | □ |
| $s_7$ | ◯ | △ | □ | empty |
| $s_8$ | ◯ | empty | □ | △ |
| $s_9$ | ◯ | △ | □ | ◇ |
| $s_{10}$ | ◯ | empty | ◯ | empty |
| $s_{11}$ | ◯ | △ | ◯ | empty |
| $s_{12}$ | ◯ | empty | ◯ | △ |
| $s_{13}$ | ◯ | △ | ◯ | □ |

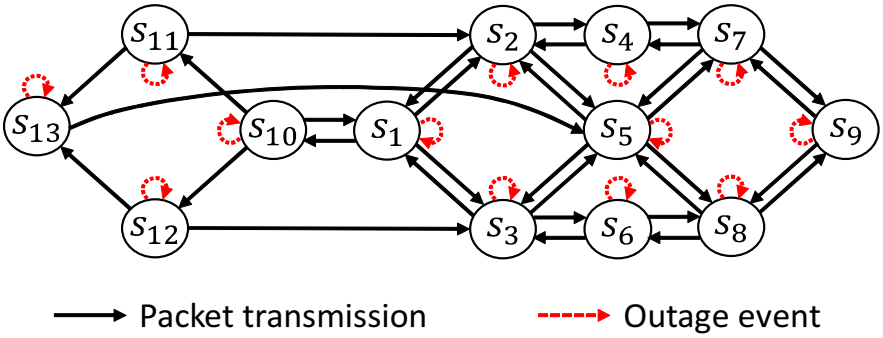


Figure 4.1: State transition diagram of the MC model representing the proposed scheme with $K = 2$ relay nodes, each having $(L = 2)$-sized buffers.

from state $s_1$ as an example, where there is no packet in both of $K = 2$ SR nodes. Based on the channel coefficients of the two SS-SR links, one of the transitions from initial state $s_1$ to states $s_2$, $s_3$ and $s_{10}$ is possible, as shown in Fig. 4.1. More specifically, either the transition from state $s_1$ to state $s_2$ or state $s_3$ occurs when only one of the two SS-SR links is activated. The transition associated with the broadcasting phase corresponds to that from state $s_1$ to state $s_{10}$, which occurs when both of the two SS-SR links are successfully activated. Next, under the assumption that the current buffer state is state $s_{10}$, either of the transitions to states $s_1$, $s_{11}$ or $s_{12}$ is possible. To be specific, the transition from state $s_{10}$ to state $s_1$ occurs when either of the two SR-SD links is activated. Note that after an ACK packet is sent to both the SR nodes, multiple copies of the corresponding packet stored in the buffers of the SR nodes are deleted from the

buffers at all the related SR nodes. Either transition from state $s_{10}$ to state $s_{11}$ or state $s_{12}$ occurs when neither of the two SR-SD links is activated but either of the two SS-SR is. Note that in state $s_{10}$, the priorities of the two SS-SR links are low, and hence the broadcasting is avoided.

## 4.2 State Transition Matrix

The set of the legitimate links and that of the available links that can successfully transmit one packet are denoted by $L_j$ and $L_j^s$, respectively, at state $s_j$. Here, we have the relationship $L_j^s \subset L_j$. Moreover, we define $U_j$ as the set of states that have the possibility of being arrived from state $s_j$ through one-step transition. Next, we calculate the state transition matrix $\mathbf{A} \in \mathbb{R}^{N_{\text{state}} \times N_{\text{state}}}$, whose $i$th-row and $j$th-column element is represented by [20]

$$\mathbf{A}_{ij} = \sum_{L_j^s \subset L_j} \Pr(L_j^s) \Pr(s_j \to s_i | L_j^s). \tag{4.1}$$

Here, the conditional probability $\Pr(s_j \to s_i | L_j^s)$ is calculated based on the link selection algorithm shown in Table 3.2. Additionally, $\Pr(L_j^s)$ is the possibility that all the links in $L_j^s$ can successfully transmit a packet, which is formulated by

$$\Pr(L_j^s) = \Pr^{\text{SS-SR}}(L_j^s) \Pr^{\text{SR-SD}}(L_j^s), \tag{4.2}$$

where $\Pr^{\text{SS-SR}}(L_j^s)$ and $\Pr^{\text{SR-SD}}(L_j^s)$ represent the possibilities that SS-SR and SR-SD links in $L_j^s$ can successfully transmit a packet, respectively. Moreover, $\Pr^{\text{SS-SR}}(L_j^s)$ of (4.2) is expressed by

$$\begin{aligned} \Pr^{\text{SS-SR}}(L_j^s) = & \prod_{l_{\text{SS-SR}_k} \in L_j^s} (1 - P_{\text{out}}^{\text{SS-SR}_k}) \\ & \prod_{l_{\text{SS-SR}_k} \notin L_j^s, l_{\text{SS-SR}_k} \in L_j} P_{\text{out}}^{\text{SS-SR}_k}, \end{aligned} \tag{4.3}$$

where $l_{a-b}$ denotes the link between node $a$ and node $b$, while $P_{\text{out}}^{\text{SS-SR}_k}$ denotes the outage probability of SS-SR$_k$ link. Besides, $\Pr^{\text{SR-SD}}(L_j^s)$ of (4.2) can be expressed similarly. As mentioned in Section 3.1, the transmission power of the SS node is designed for satisfying the power constraint of $P_{\text{SS}}\gamma_{\text{SS-PD}} \leq I_{\text{th}}$. Hence, the SIR of SS-SR$_k$ links has $\gamma_{\text{SS-PD}}$, as shown in (3.3). Additionally, the SIR of SR$_k$-SD links contains $\gamma_{\text{PS-SD}}$, as showin in (3.4), since all the SR$_k$-SD link suffer from the same interference from the PS node. We note that $\gamma_{\text{SS-PD}}$ and $\gamma_{\text{PS-SD}}$ result in a correlation among different links, which contradicts the assumption of independent channels [13, 38, 39]. However, for the sake of simplicity, we assume that SS-SR links are mutually independent, and so do the SR-SD links in our theoretical analysis.

## 4.3 Theoretical Bound of Outage Probability

Since the derivation of the outage probability of the SS-SR links and that of the SR-SD links are similar, the former is provided in this section. Based on the definition of the

outage probability, $P_{\text{out}}^{\text{SS-SR}_k}$ is formulated by

$$\begin{aligned} P_{\text{out}}^{\text{SS-SR}_k} &= \Pr(C_{\text{SS-SR}} < r_0) \\ &= \Pr(\frac{1}{2}\log_2\left(1+\frac{I_{\text{th}}\gamma_{\text{SS-SR}_k}}{\gamma_{\text{SS-PD}}\gamma_{\text{PS-SR}_k}}\right) < r_0), \end{aligned} \tag{4.4}$$

where $r_0$ denotes the transmission rate of each link. Furthermore, letting $x_k = I_{\text{th}}\gamma_{\text{SS-SR}_k}/\gamma_{\text{PS-SR}_k}$ and $y_k = x_k/\gamma_{\text{SS-PD}}$, we have

$$\begin{aligned} P_{\text{out}}^{\text{SS-SR}_k} &= \Pr(y_k < 2^{2r_0}-1) \\ &= F_{Y_k}(y_k = 2^{2r_0}-1), \end{aligned} \tag{4.5}$$

where $F_{Y_k}(y_k)$ is the cumulative distribution function (CDF) of $y_k$. Since $\gamma_{\text{SS-SR}_k}$ and $\gamma_{\text{PS-SR}_k}$ are exponentially distributed and mutually independent, the CDF of $x_k$ can be obtained as

$$\begin{aligned} F_{X_k}(x_k) &= \Pr\left(\frac{I_{\text{th}}\gamma_{\text{SS-SR}_k}}{\gamma_{\text{PS-SR}_k}} \leq x_k\right) \\ &= \frac{x_k\lambda_{\text{PS-SR}_k}}{I_{\text{th}}\lambda_{\text{SS-SR}_k} + x_k\lambda_{\text{PS-SR}_k}}. \end{aligned} \tag{4.6}$$

Here, $\lambda_{a\text{-}b}$ indicates the average channel gain of the link $l_{a\text{-}b}$, i.e., $\mathbb{E}[\gamma_{a\text{-}b}] = \lambda_{a\text{-}b}$. Since $\gamma_{\text{SS-PD}}$ is exponentially distributed and independent of $x_k$, from (4.6), the CDF of $y_k$ is expressed by

$$\begin{aligned} F_{Y_k}(y_k) &= \int_0^\infty \frac{1}{\lambda_{\text{SS-PD}}} e^{-\frac{\gamma_{\text{SS-PD}}}{\lambda_{\text{SS-PD}}}} \cdot \frac{y_k\gamma_{\text{SS-PD}}}{\lambda_{ratio}^{\text{SS-SR}_k} + y_k\gamma_{\text{SS-PD}}} \mathrm{d}\gamma_{\text{SS-PD}} \\ &= 1 - \frac{\lambda_{ratio}^{\text{SS-SR}_k}}{\lambda_{\text{SS-PD}}y_k} e^{\frac{\lambda_{ratio}^{\text{SS-SR}_k}}{\lambda_{\text{SS-PD}}y_k}} \text{Ei}\left(\frac{\lambda_{ratio}^{\text{SS-SR}_k}}{\lambda_{\text{SS-PD}}y_k}\right), \end{aligned} \tag{4.7}$$

where $\text{Ei}(x) = \int_x^\infty (e^{-t}/t)\mathrm{d}t$ and $\lambda_{ratio}^{\text{SS-SR}_k} = I_{\text{th}}\lambda_{\text{SS-SR}_k}/\lambda_{\text{PS-SR}_k}$. By substituting (4.7) into (4.5), we obtain $P_{\text{out}}^{\text{SS-SR}_k}$. Also, we have $\Pr^{\text{SS-SR}}(L_j^s)$, by substuting $P_{\text{out}}^{\text{SS-SR}_k}$ into (4.3). As mentioned above, $\Pr^{\text{SR-SD}}(L_j^s)$ of (4.2) is obtained in a similar manner. Hence, we arrive at all the elements of the state transition matrix $\mathbf{A}_{ij}$ from (4.1). Finally, we have

$$\mathbf{A}_{jj} = \prod_{l_{\text{SS-SR}_k} \in L_j} P_{\text{out}}^{\text{SS-SR}_k} \prod_{l_{\text{SR}_k\text{-SD}} \in L_j} P_{\text{out}}^{\text{SR}_k\text{-SD}}. \tag{4.8}$$

Again, we assume that the SS-SR links are independent of each other, and the same assumption is also employed for the SR-SD links. Hence, $\text{A}_{jj}$ is formulated by the formulation shown in (4.8). In conclusion, the elements of the state transition matrix $\mathbf{A}$ are given by

$$\mathbf{A}_{ij} = \begin{cases} 0 & if\ s_i \notin U_j \\ (P_{\text{out}}^{\text{SS-SR}_k})^{N_j^{\text{SS-SR}}} (P_{\text{out}}^{\text{SR}_k\text{-SD}})^{N_j^{\text{SR-SD}}} & if\ s_i \in U_j, i = j \\ \sum_{S_j^{\text{SS-SR}}=0}^{N_j^{\text{SS-SR}}} \sum_{S_j^{\text{SR-SD}}=0}^{N_j^{\text{SR-SD}}} a_{ij} & if\ s_i \in U_j, i \neq j \end{cases}$$

$$\text{for } i, j \in \{1, \cdots, N_{\text{state}}\}, \tag{4.9}$$

where $N_j^{a\text{-}b}$ and $S_j^{a\text{-}b}$ denote the total number of the legitimate links and the number of available links that can successfully transmit a packet from node $a$ to node $b$ at state $s_j$, respectively. Furthermore, $S_j^{\text{SS-SR}}$ and $S_j^{\text{SR-SD}}$ are the numbers of available SS-SR and SR-SD links which can successfully deliver a packet, respectively. When $S_j^{\text{SS-SR}} = S_j^{\text{SR-SD}} = 0$, then we have $a_{ij} = 0$. Otherwise,

$$\begin{aligned} a_{ij} &= \binom{N_j^{\text{SS-SR}}}{S_j^{\text{SS-SR}}} (1 - P_{\text{out}}^{\text{SS-SR}_k})^{S_j^{\text{SS-SR}}} (P_{\text{out}}^{\text{SS-SR}_k})^{N_j^{\text{SS-SR}} - S_j^{\text{SS-SR}}} \\ &\times \binom{N_j^{\text{SR-SD}}}{S_j^{\text{SR-SD}}} (1 - P_{\text{out}}^{\text{SR}_k\text{-SD}})^{S_j^{\text{SR-SD}}} (P_{\text{out}}^{\text{SR}_k\text{-SD}})^{N_j^{\text{SR-SD}} - S_j^{\text{SR-SD}}} \\ &\times \Pr(s_j \to s_i | L_j^s), \end{aligned} \tag{4.10}$$

where $\binom{N}{S} = \frac{N!}{S!(N-S)!}$.

*Proposition 1:* the Markov chain model of the proposed scheme is irreducible and aperiodic.

*Proof:* Due to the structure of the problem considered, it is possible for any legitimate buffer state to transfer to all other states, and hence the Markov chain model considered is irreducible. Additionally, as mentioned above, $\mathbf{A}_{jj}$ corresponds to the outage probability at state $s_j$, where the buffer state remains unchanged. Since $\mathbf{A}_{jj} > 0$ ($j \in \{1, \cdots, N_{\text{state}}\}$), the probability of staying at any legitimate state after $N$ and $N+1$ transitions is higher than zero. Hence, the Markov chain model considered is aperiodic.

According to [17], since the Markov chain model of the proposed scheme is irreducible and aperiodic, the stationary distribution vector $\boldsymbol{\pi} \in \mathbb{R}^{N_{\text{state}}}$ can be expressed by

$$\boldsymbol{\pi} = (\mathbf{A} - \mathbf{I} + \mathbf{B})^{-1}\mathbf{b}, \tag{4.11}$$

where $\mathbf{B} \in \mathbb{R}^{N_{\text{state}} \times N_{\text{state}}}$ is a matrix with all elements to be one, and $\mathbf{b} = [1, \cdots, 1]^T \in \mathbb{R}^{N_{\text{state}}}$, while $\mathbf{I} \in \mathbb{R}^{N_{\text{state}} \times N_{\text{state}}}$ is the identity matrix. Thus, the outage probability of the whole system can be obtained as [17]

$$P_{\text{out}} = \text{diag}(\mathbf{A})\boldsymbol{\pi}. \tag{4.12}$$

## 4.4 Theoretical Bound of Average Packet Delay

Based on Little's law [40], the average packet delay at the $\text{SR}_k$ node is expressed by

$$\mathbb{E}[T_k] = \frac{\mathbb{E}[\Psi_k]}{\eta_k}, \tag{4.13}$$

where $\eta_k$ denotes the average throughput of the $\text{SR}_k$ node. According to [18], the average packet delay of each SR node is also the same as (4.13), since the probabilities of selecting any of the SR nodes are assumed to be identical. More specifically, since the independent and identically distributed Rayleigh fading channels are considered in our

system model, $\eta_k$ is identical for each SR node, which can be approximately expressed as $\eta_k = (1 - P_{\text{out}})/2$ [20], hence (4.13) is modified to

$$\mathbb{E}[T_k] = \frac{2}{1 - P_{\text{out}}} \sum_{i=1}^{N_{\text{state}}} \boldsymbol{\pi}_i \Psi_k(i), \tag{4.14}$$

where $\boldsymbol{\pi}_i$ denotes the $i$-th element of the stationary distribution vector $\boldsymbol{\pi}$, and $\Psi_k(i)$ is the total number of different packets stored in the buffers of all the SR nodes at state $s_i$.

## 4.5 Diversity Order

In this section, the diversity order is analyzed, which is given by

$$d = -\lim_{\lambda \to \infty} \frac{\log P_{\text{out}}}{\log \lambda}, \tag{4.15}$$

where $\lambda$ is the average channel gain. Here, we divide all the buffer states into two categories. The first category contains all the buffer states where the buffers of all the relay nodes are neither full nor empty, while the second category contains all the buffer states where at least one of the relay buffers is either full or empty. If we define the set of states in the first and secondary category by $F_1$ and $F_2$, it is obvious that there are $2K$ available links if the buffer state $s_n \in F_1$, and the number of the available links is less than $2K$ if the buffer state $s_n \in F_2$. We herein consider the case where each relay node has infinite-sized buffers ($L \to \infty$), the outage probability can be rewritten as [20]

$$P_{\text{out}} = \sum_{s_n \in F_1} \boldsymbol{\pi}_n \mathbf{A}_{nn} + \sum_{s_n \in F_2} \boldsymbol{\pi}_n \mathbf{A}_{nn}. \tag{4.16}$$

Since $\lim_{L\to\infty} \boldsymbol{\pi}_n = 0$ when $s_n \in F_2$ [20], (4.16) can be simplified as

$$P_{\text{out}} = \sum_{s_n \in F_1} \boldsymbol{\pi}_n \mathbf{A}_{nn} (L \to \infty). \tag{4.17}$$

We consider the independent and identically distributed channels here, and let $\lambda_{\text{SS-SR}_k} = \lambda_{\text{SR}_k\text{-SD}} = \lambda$, $\lambda_{\text{SS-PD}} = \lambda_{\text{PS-SR}_k} = \lambda_{\text{PS-SD}} = \lambda_{\text{SR}_k\text{-PD}} = \lambda_{int}$. Hence, $\lambda_{ratio}^{\text{SS-SR}_k} = \lambda_{ratio}^{\text{SR}_k - \text{SD}} = I_{\text{th}}\lambda/\lambda_{int}$. According to (4.5) and (4.7), we can further have $P_{\text{out}}^{\text{SS-SR}_k} = P_{\text{out}}^{\text{SR}_k\text{-SD}}$. If we denote $P_{\text{out}}^{\text{SS-SR}_k}$ and $P_{\text{out}}^{\text{SR}_k\text{-SD}}$ as $P_{\text{out}}^{link}$, then we have $\mathbf{A}_{nn} = (P_{\text{out}}^{link})^{2K}$, since there are $2K$ available links if the buffer state $s_n \in F_1$. Hence, since $\sum_{n=1}^{N_{state}} \boldsymbol{\pi}_n = 1$ and $\lim_{L\to\infty} \boldsymbol{\pi}_n = 0$ when $s_n \in F_2$, (4.17) can be rewritten as $P_{\text{out}} = \sum_{s_n \in F_1} \boldsymbol{\pi}_n (P_{\text{out}}^{link})^{2K} = (P_{\text{out}}^{link})^{2K} (L \to \infty)$. Then, on the basis of (4.5) and (4.7), the outage probability can be given by

$$P_{\text{out}} = [F_{Y_k}(y_k = 2^{2r_0} - 1)]^{2K} (L \to \infty). \tag{4.18}$$

For convenience, we here denote the constant term $\frac{I_{\text{th}}}{\lambda_{int}^2 \cdot y_k}$ by $C$. Hence, (4.15) can be given as

$$d = -\lim_{\lambda \to \infty} \frac{\log[(F_{Y_k}(y_k = 2^{2r_0} - 1))^{2K}]}{\log \lambda}$$

$$
\begin{aligned}
&= -\lim_{\lambda\to\infty} \frac{2K\log(1 - C\lambda e^{C\lambda}\int_{C\lambda}^{\infty}\frac{e^{-t}}{t}dt)}{\log\lambda} \\
&= -\lim_{\lambda\to\infty} \frac{2K\log(1 - \frac{C\int_{C\lambda}^{\infty}\frac{e^{-t}}{t}dt}{\frac{1}{\lambda e^{C\lambda}}})}{\log\lambda} \\
&= -\lim_{\lambda\to\infty} \frac{2K\log(1 - \frac{-Ce^{-C\lambda}\times C}{-\frac{1}{\lambda^2 e^{C\lambda}} - \frac{C}{\lambda e^{C\lambda}}})}{\log\lambda} \\
&= -\lim_{\lambda\to\infty} \frac{2K\log(1 - \frac{C\lambda}{1+C\lambda})}{\log\lambda} \\
&= -\lim_{\lambda\to\infty} \frac{2K(-\log(1+C\lambda))}{\log\lambda}. \\
&= 2K. \qquad (4.19)
\end{aligned}
$$

Here, note that the diversity order is analyzed under the assumption that each SR node has the infinite-sized buffers, and the analytical outage probability $P_{out}$ is derived by ignoring the correlation problem mentioned in Section 4.3. As a result, the derived diversity order in (4.19) corresponds to the upper-bound of the proposed scheme.

## 4.6 Overhead Required for CSI and Buffer States

Table 4.2: Required overheads of the max-ratio scheme and the proposed scheme for the SD node at each time slot.

| | Pilot transmissions | | | CSI estimations | | | Data transmissions from SR nodes | |
|---|---|---|---|---|---|---|---|---|
| | SS node | each SR node | PD node | SS node | each SR node | SD node | CSI of SS-SR links | buffer states |
| Max-ratio scheme [13] | 1 | 1 | 1 | 1 | 2 | $K$ | $K$ | $K$ |
| Proposed GBSB scheme | 1 | 1 | 1 | 1 | 2 | $K$ | $K$ | $K$ |

The overheads required for the link selection of the max-ratio scheme and the proposed scheme are investigated here. In the proposed scheme, CSI and the buffer states of the relay nodes are needed at the SD node, which acts as the central coordinator in our system model, in order to achieve the link selection at each time slot. Hence, We herein focus on the required overheads for monitoring the CSI and buffer states. The required overheads are shown in Table 4.2, which lists the number of pilot transmissions, CSI estimations, and the data transmissions from SR nodes during each time slot, the same evaluation criterion as in [21]. In the proposed scheme, the CSI of all the SS-SR and SR-SD links should be updated at the SD node during each time slot before link selection, which is also necessary for the max-ratio scheme. More specifically, the SS node first broadcasts a pilot block to all the SR nodes, and each SR node estimates the CSI of the corresponding SS-SR link based on the received pilot block. Next, the estimated CSI at each SR node, together with the buffer states, is transmitted to the SD node. Then, each SR node transmits a pilot block to the SD node, and SD node then conducts the CSI estimation of $K$ SR-SD links based on the received $K$ pilot blocks. As mentioned in Section 3.1, the PD node broadcasts a pilot block to the SS node and all the SR nodes at each time slot. Then, the SS node and the SR nodes carry out the CSI estimation of

PD-SS and PD-SR links, respectively, so that the transmission nodes in the secondary network can adjust their transmission power. As for the max-ratio scheme, the numbers of the required overheads considered here are the same as the proposed scheme. It is worth mentioning that in the max-ratio scheme, the SD node collects the partial buffer state information, which is binary (full or empty), while in the proposed scheme, the complete buffer state information is collected. As a result, the overhead of the proposed scheme may become more extensive than that of the max-ratio scheme.

## 4.7 Theoretical Results and Discussions

In this section, the theoretical results are presented and compared with the numerical results, in order to validate our theoretical analysis. Specifically, we examined the outage probability and average packet delay of the proposed scheme with system parameters $(K, L) = (1, 2)$, $(1, 5)$, $(2, 1)$ and $(2, 2)$, respectively. Parameters used in the simulations are shown in Table 5.1, while we set $(\xi_{\text{SS-SR}}, \xi_{\text{SR-SD}}) = (0, 2)$ when $L = 2$. The effects of $\xi_{\text{SS-SR}}$ and $\xi_{\text{SR-SD}}$ on the outage probability and average packet delay are presented in the Section 5.1, which enables us to determine the values of $\xi_{\text{SS-SR}}$ and $\xi_{\text{SR-SD}}$.

### 4.7.1 Outage probability

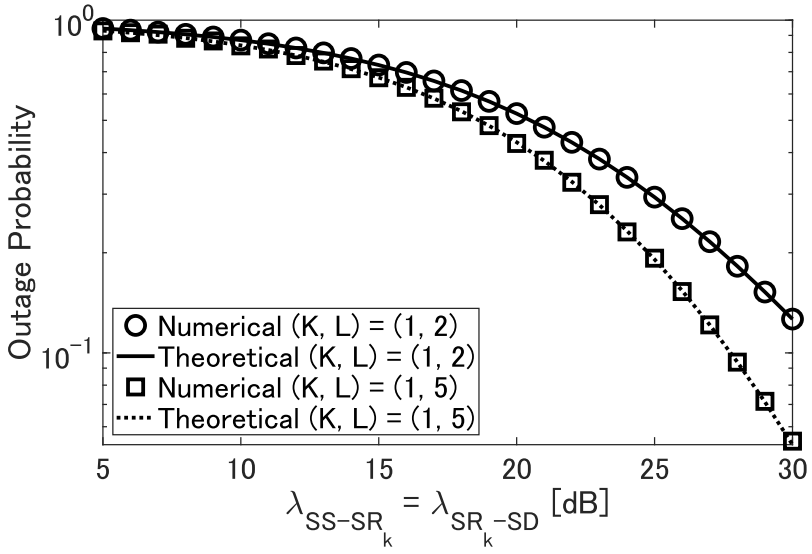


Figure 4.2: Theoretical and numerical outage probability of the proposed scheme with the system parameters $(K, L) = (1, 2)$ and $(1, 5)$.

The theoretical outage probabilities are presented here. Fig. 4.2 shows the theoretical and numerical curves of the proposed scheme with the parameters of $(K, L) = (1, 2)$ and $(1, 5)$. It was found that both the curves coincided. Recall that our theoretical analysis is based on the assumption of mutually independent SS-SR and SR-SD links. Note that for the scenario of a $K = 1$ SR node, the number of SS-SR links and that of SR-SD links is one. Hence, the correlation mentioned above problem does not exist.

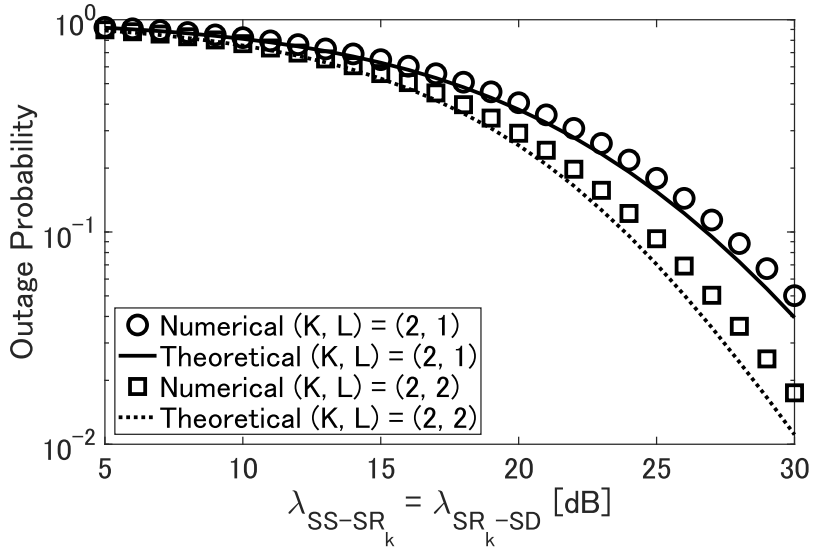


Figure 4.3: Theoretical and numerical outage probability of the proposed scheme with the system parameters $(K, L) = (2, 1)$ and $(2, 2)$.

Next, Fig. 4.3 shows the theoretical and numerical curves for $(K, L) = (2, 1)$ and $(2, 2)$. Observe in Fig. 4.3 that there is a slight gap between the theoretical and numerical curves for each $(K, L)$ scenario. For $K = 2$, there is a correlation between $K = 2$ SS-SR links and that between $K = 2$ SR-SD links, and it was found that the effects of such correlation problem may slightly degrade the achievable performance. In our theoretical analysis, it is assumed that the SS-SR links are independent of each other for simplicity, and the same assumption is also employed for the SR-SD links. However, the SS-SR links are actually dependent with each other, while, similarly, SR-SD links are. As a result, a slight gap exists between the numerical and theoretical results for $K \geq 2$, since the theoretical analysis does not take into account the effects of the correlation, unlike in the numerical analysis. More specifically, when $K = 1$, there is no link selection and the numerical results matched well with the theoretical results, because of the absence of the correlation problem, as shown in Fig. 4.2. However, for $K \geq 2$, there exists multiple SS-SR links and multiple SR-SD links, hence exhibiting a slight gap between the numerical and theoretical results, as shown in Fig. 4.3.

### 4.7.2 Average packet Delay

The theoretical average packet delays are presented here. Fig. 4.4 shows the theoretical and numerical curves of the proposed scheme with the parameters $(K, L) = (1, 2)$ and $(1, 5)$. In each scenario, the theoretical and numerical curves agreed well. Furthermore, in Fig. 4.5, the system parameters were changed to $(K, L) = (2, 1)$ and $(2, 2)$. In a similar manner to the above-mentioned outage probability analysis, the theoretical average delay is slightly different from the numerical one. As mentioned in Section 4.7.1, for $K = 2$, the correlation problem gave rise to the differences between the numerical and theoretical average packet delays.

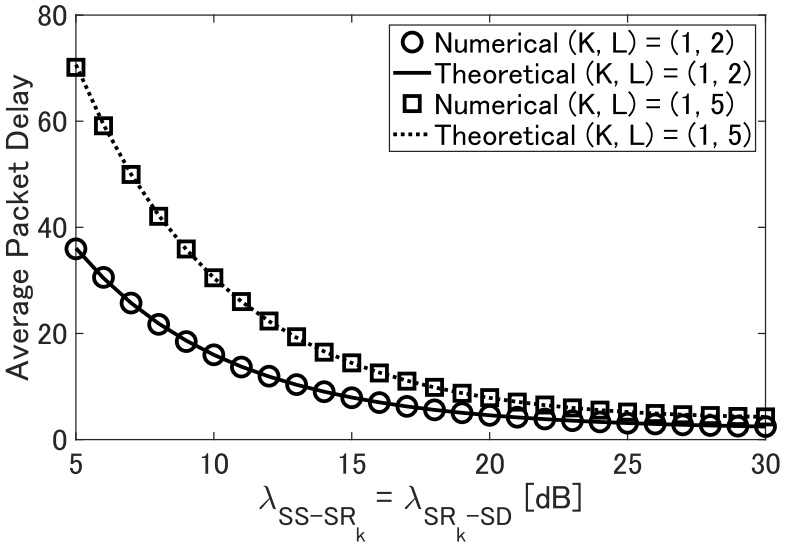


Figure 4.4: Theoretical and numerical average packet delay of the proposed scheme with the system parameters $(K, L) = (1, 2)$ and $(1, 5)$.

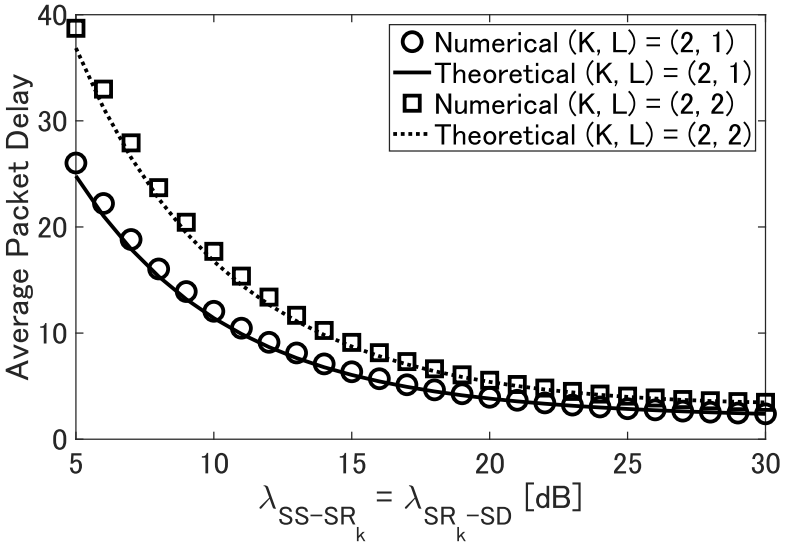


Figure 4.5: Theoretical and numerical average packet delay of the proposed scheme with the system parameters $(K, L) = (2, 1)$ and $(2, 2)$.

## 4.8 Summary

Theoretical outage probabilities, as well as the average packet delay， are analyzed in this chapter, based on the Markov chain model. Besides, the analysis of the diversity order and the required overhead are also presented. For the scenario of one relay node, the curves of the theoretical and numerical results of both the outage probability and average packet delay coincided. However, for the scenario of multiple relay nodes, there are some gaps between the theoretical and numerical results. This is because our theoretical analysis is based on the assumption that the SS-SR links are independent of each other for simplicity, and the same assumption is also employed for the SR-SD links, while the numerical analysis takes into account the dependence of the SS-SR and SR-SD links.

# Chapter 5

# Numerical Analysis of GBSB Relay Selection

In this section, we provide the numerical results of the outage probability and average packet delay of the proposed scheme, in order to characterize the achievable performance of the proposed scheme and compare the performance with the benchmark scheme. Here, the max-ratio relay selection scheme [13] was selected as the benchmark scheme. Throughout the simulations, the transmission rate was fixed to $r_0 = 1$ [bps/Hz]. Furthermore, the predefined level $I_{\text{th}}$ and the transmission power of the PS node were set to unity. In the initial condition of each Monte Carlo simulation, the buffers of all the SR nodes were set to empty, and $10^6$ source packets were generated at the SS node.

Table 5.1: System Parameters in the Simulations

| | |
|---|---|
| Channel | Quasi-static Rayleigh fading |
| Relay | half-duplex & decode-and-forward |
| Secondary source packets | $10^6$ |
| Fixed transmission rate | 1 [bps/Hz] |
| Predefined level $I_{\text{th}}$ | 30 [dBm] |
| Transmission power of PS node | 30 [dBm] |
| $\lambda_{\text{SS-PD}} = \lambda_{\text{PS-SR}_k} = \lambda_{\text{PS-SD}} = \lambda_{\text{SR}_k\text{-PD}}$ | 10 dB |
| $\xi_{\text{SS-SR}}$ | 1 when $L \geq 3$ |
| $\xi_{\text{SR-SD}}$ | 2 when $L \geq 3$ |

## 5.1 Effects of Parameter $\xi_{\text{SS-SR}}$ and $\xi_{\text{SR-SD}}$

Here, the effects of parameter $\xi_{\text{SS-SR}}$ and $\xi_{\text{SR-SD}}$ are presented. This investigation is helpful for us to determine the values of these two parameters and keep the balance between the outage probability and average packet delay, in order to achieve the ideal system performance. Fig. 5.1 shows the effects of the thresholding parameter $\xi_{\text{SS-SR}}$ on the outage probability and average packet delay with the system parameter $(K, L) = (5, 10)$ and $\xi_{\text{SR-SD}} = 2$. As shown in Fig. 5.1(a), there was a relatively obvious gap between the curve of $\xi_{\text{SS-SR}} = 0$ and 1. However, the gap became marginal when $\xi_{\text{SS-SR}}$ became larger. This is because a larger value of $\xi_{\text{SS-SR}}$ means an increase in the number of available SS-SR links with the highest priority, which increases the possibility of the activation of the broadcasting phase, and can attain higher diversity gain in the relaying phase. However, this improvement is limited, especially when the number

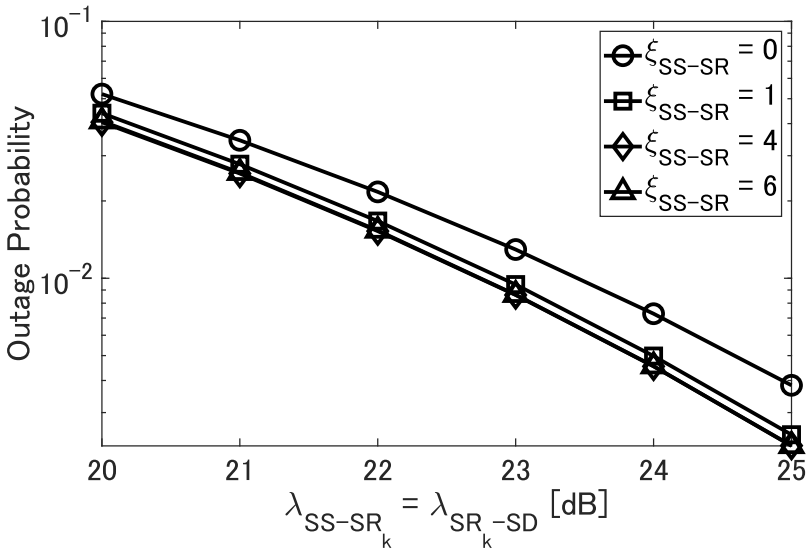


(a)

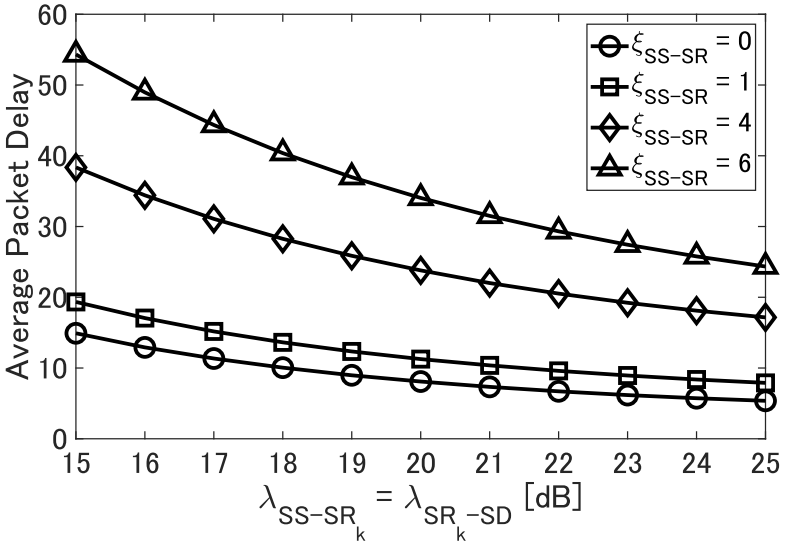


(b)

Figure 5.1: Effects of parameter $\xi_{\text{SS-SR}}$ on the outage probability and average packet delay with the system parameter $(K, L) = (5, 10)$ and $\xi_{\text{SR-SD}} = 2$.

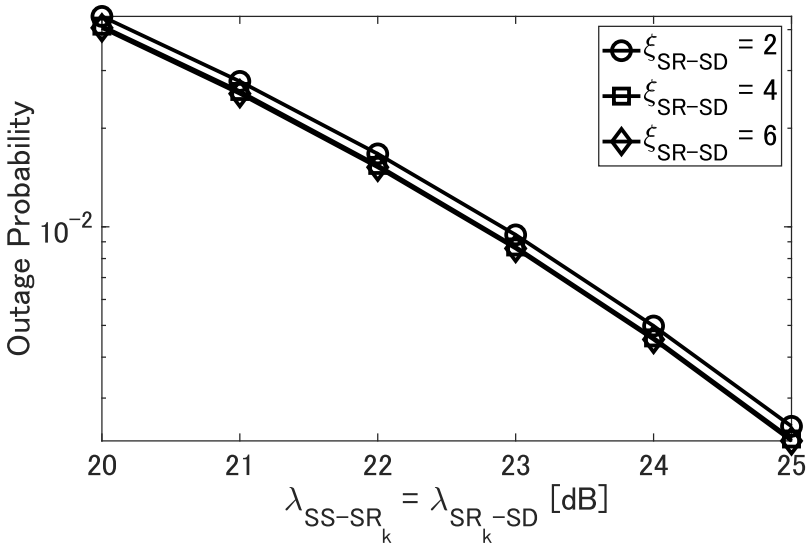


(a)

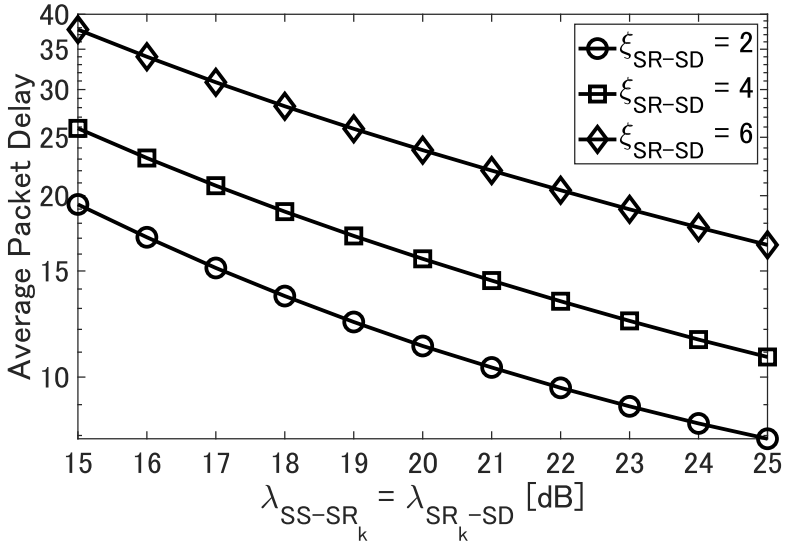


(b)

Figure 5.2: Effects of parameter $\xi_{\text{SR-SD}}$ on the outage probability and average packet delay with the system parameter $(K, L) = (5, 10)$ and $\xi_{\text{SS-SR}} = 1$.

of available links is large enough. In contrast, there was an obvious deterioration in the packet-delay performance with an increasing $\xi_{\text{SS-SR}}$, as Fig. 5.1(b) shows, since a larger value of $\xi_{\text{SS-SR}}$ means the reduction of the number of available SS-SR links, which imposes the negative effect on the end-to-end packet delay. In conclusion, the above simulation results show that although a lower value of $\xi_{\text{SS-SR}}$ resulted in the worse outage performance, this deterioration was limited. However, a lower value of $\xi_{\text{SS-SR}}$ could contribute to the obvious reduction in terms of the average packet delay. Hence, $\xi_{\text{SS-SR}} = 1$ was ideal for us to achieve low average packet delay, while maintaining a good outage performance, compared to other values of $\xi_{\text{SS-SR}}$. Next, the effects of parameter $\xi_{\text{SR-SD}}$ were investigated. As Fig. 5.2 shows, the effects of the thresholding parameter $\xi_{\text{SR-SD}}$ on the outage probability and average packet delay were similar to that of the thresholding parameter $\xi_{\text{SR-SD}}$, since a lower $\xi_{\text{SR-SD}}$ reduces the number of packets stored at the relay nodes, while also leads to the reduction of available SR-SD links. Hence, we set $\xi_{\text{SR-SD}} = 2$ in consideration of both the outage performance and the packet-delay performance. Note that when $L = 2$, all available SS-SR links are categorized into the group with the highest priority if $\xi_{\text{SS-SR}} = 1$. As a result, we consider $(\xi_{\text{SS-SR}}, \xi_{\text{SR-SD}}) = (0, 2)$ when $L = 2$, in order to classify all available SS-SR links into two different groups with the highest priority and low priority, and set $(\xi_{\text{SS-SR}}, \xi_{\text{SR-SD}}) = (1, 2)$ when $L \geq 3$.

## 5.2 Numerical Outage Probability

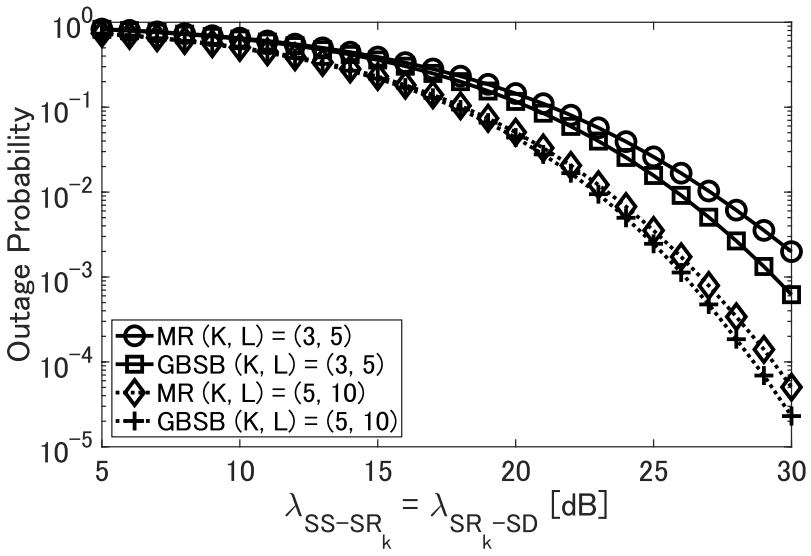


Figure 5.3: Outage-probability comparisons between the max-ratio scheme [13] and the proposed scheme with the system parameters $(K, L) = (3, 5)$ and $(5, 10)$.

Firstly, Fig. 5.3 shows the outage probability of the two schemes, having the system parameters $(K, L) = (3, 5)$ and $(5, 10)$. $\lambda_{\text{SS-SR}_k} = \lambda_{\text{SR}_k\text{-SD}}$ $(k \in \{1, ..., K\})$ were varied from 5 to 30 dB with a step of 1 dB. Observe in Fig. 5.3 that the proposed scheme outperformed the max-ratio relay selection scheme, where the performance gap increased,

upon increasing the $\lambda_{\text{SS-SR}_k}$ and $\lambda_{\text{SR}_k-\text{SD}}$. This is mainly because the proposed scheme takes into account the buffer states for the link selection, while the max-ratio relay selection scheme does not. Hence, the proposed scheme is capable of maximizing the number of available links by reducing the probabilities of the empty and full buffer states.

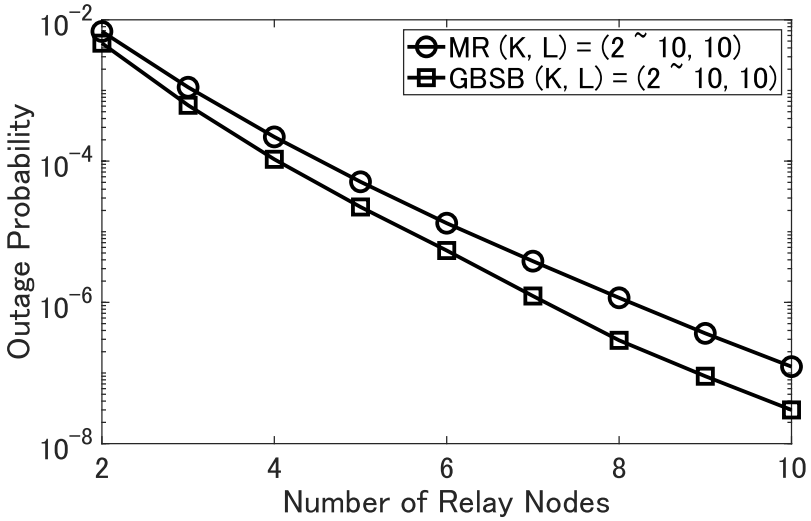


Figure 5.4: Outage probability versus the number of SR nodes $K$, where we considered $L = 10$, while the number of SR nodes was varied from $K = 2$ to $K = 10$.

Next, in Fig. 5.4 we investigated the effects of the number of SR nodes on the outage probability of the two schemes, respectively. The average SIRs of the SR and SD nodes were set to $\lambda_{\text{SS-SR}_k} = \lambda_{\text{SR}_k-\text{SD}} = 30$ dB. The buffer size of each relay node was set to $L = 10$, and the number of the SR nodes was varied from $K = 2$ to $K = 10$. Observe in Fig. 5.4 that when the number of the SR nodes increased, the outage performance improved in both the schemes, since the number of SR nodes was directly associated with the maximum achievable diversity gain. The performance advantage of the proposed scheme over the conventional max-ratio counterpart increased, upon increasing the number of SR nodes.

## 5.3 Numerical Average Packet Delay

Next, the numerical results of the average packet delay are presented. In this thesis, the average packet delay represents the average number of time slots that is required for each secondary source packet to arrive at the SD node. In Fig. 5.5, we evaluated the effects of $\lambda_{\text{SS-SR}_k}$ and $\lambda_{\text{SR}_k-\text{SD}}$ on the average end-to-end packet delay, where we considered the system parameters $(K, L) = (3, 5)$ and $(5, 10)$. Additionally, $\lambda_{\text{SS-SR}_k} = \lambda_{\text{SR}_k-\text{SD}}$ $(k \in \{1, ..., K\})$ were varied from 5 to 30 dB with a step of 1 dB. As seen in Fig. 5.5, in both the schemes, the average packet delay decreased, upon increasing the $\lambda_{\text{SS-SR}_k}$ and $\lambda_{\text{SR}_k-\text{SD}}$. Moreover, the average packet delay of the proposed scheme was lower than that of the max-ratio relay selection scheme, and the relative advantage of the proposed scheme increased, upon increasing the average gain.

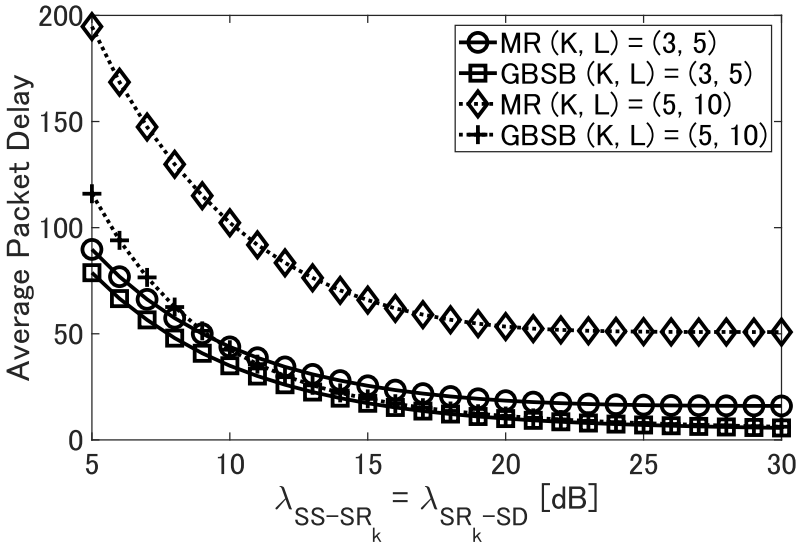


Figure 5.5: Comparisons of the packet-delay performance between the max-ratio scheme [13] and the proposed scheme with the system parameters $(K, L) = (3, 5)$ and $(5, 10)$.

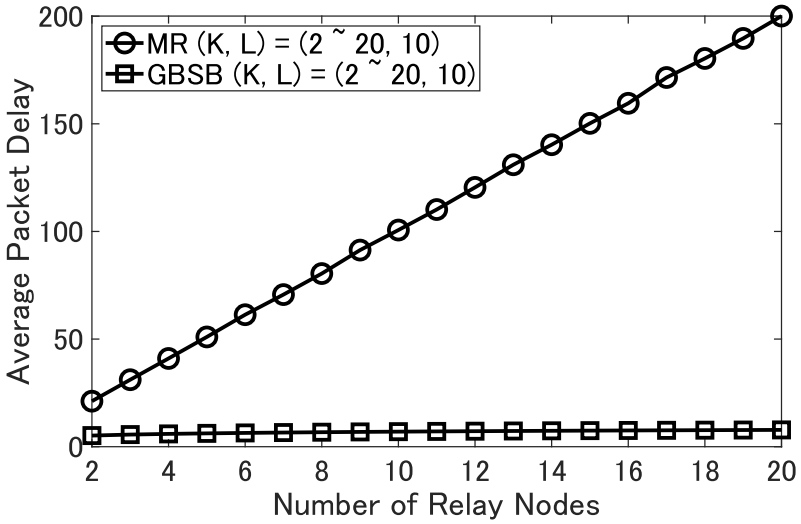


Figure 5.6: Average packet delay versus the number of the SR nodes, where we set $L = 10$, and the number of SR nodes was varied from $K = 2$ to $K = 20$.

Next, Fig. 5.6 shows the packet-delay profiles of the two schemes, where the buffer size was maintained to be $L = 10$ while varying the number of the SR nodes from $K = 2$ to $K = 20$. Besides, $\lambda_{\text{SS-SR}_k}$ and $\lambda_{\text{SR}_k-\text{SD}}$ were set to 30 dB. As shown in Fig. 5.6, the packet delay of the max-ratio relay selection scheme linearly increased, upon increasing the number of SR nodes. By contrast, the packet delay of the proposed scheme remained sufficiently low, which was approximately 5 for $K = 5$ and 8 for $K = 20$.

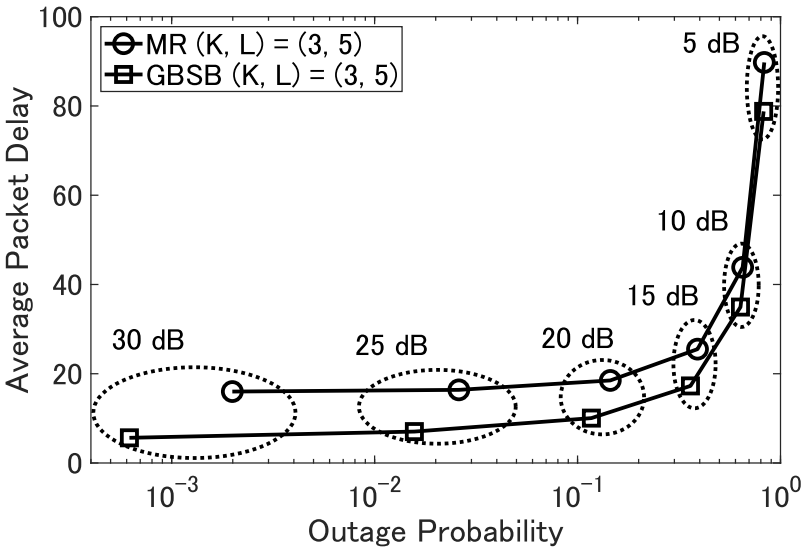


Figure 5.7: Average packet delay and outage probability of the max-ratio scheme [13] and the proposed scheme, having $K = 3$ SR nodes with a buffer of $L = 5$. $\lambda_{\text{SS-SR}_k} = \lambda_{\text{SR}_k-\text{SD}}$ ($k \in \{1, ..., K\}$) were varied from 5 to 30 dB.

Finally, Fig. 5.7 shows the outage probability and average packet delay of the two schemes. Here, we consider $K = 3$ SR nodes, each equipped with a buffer size of $L = 5$, and $\lambda_{\text{SS-SR}_k} = \lambda_{\text{SR}_k-\text{SD}}$ ($k \in \{1, ..., K\}$) were varied from 5 to 30 dB. Observe in Fig. 5.7 that while the gap between the two schemes was marginal for the low value of $\lambda_{\text{SS-SR}_k}$ and $\lambda_{\text{SR}_k-\text{SD}}$, the advantage of the proposed scheme gradually increased upon increasing the $\lambda_{\text{SS-SR}_k}$ and $\lambda_{\text{SR}_k-\text{SD}}$. However, in terms of the average packet delay, the proposed scheme outperformed the max-ratio scheme in the entire channel-gain regime.

## 5.4 Effects of Asymmetric Channels

We herein investigated the effects of the asymmetric channels, where we have $\lambda_{\text{SS-SR}_k} \neq \lambda_{\text{SR}_k\text{-SD}}$ ($k \in \{1, ..., K\}$). Here, we maintained $\lambda_{\text{SR}_k\text{-SD}} = 20$ dB, while $\lambda_{\text{SS-SR}_k}$ was varied from 10 to 30 dB with a step of 1 dB.

Fig. 5.8 shows the outage probability of the max-ratio and the proposed schemes. As shown in Fig. 5.8, the outage performance of the proposed scheme was better than that of the max-ratio scheme for $(K, L) = (3, 5)$ and $(5, 10)$. The outage probability of the proposed scheme decreased upon increasing the value of $\lambda_{\text{SS-SR}_k}$, while that of the max-ratio scheme exhibited an error floor. This is because in the max-ratio scheme the SS-SR and the SR-SD links tend to be activated for $\lambda_{\text{SS-SR}_k} > \lambda_{\text{SR}_k\text{-SD}}$ and for

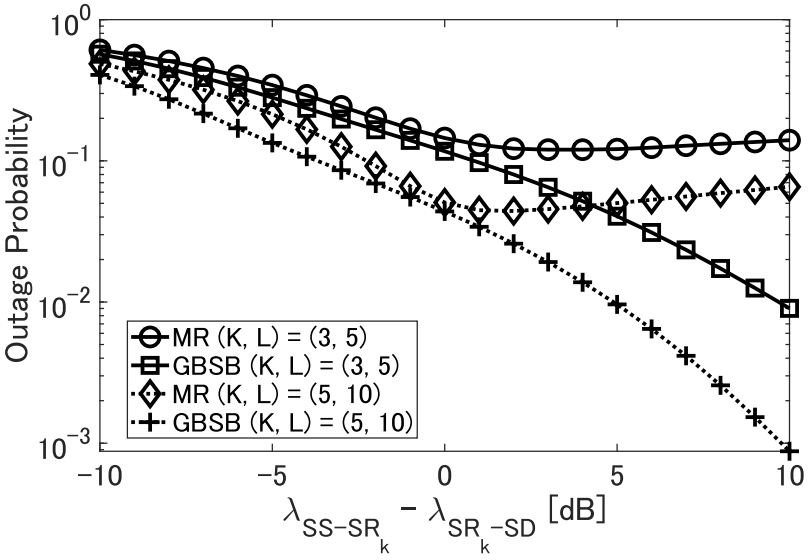


Figure 5.8: Outage probability of the max-ratio scheme [13] and the proposed scheme, where $\lambda_{\mathrm{SR}_k\text{-SD}}$ was maintained to be $\lambda_{\mathrm{SR}_k\text{-SD}} = 20$ dB.

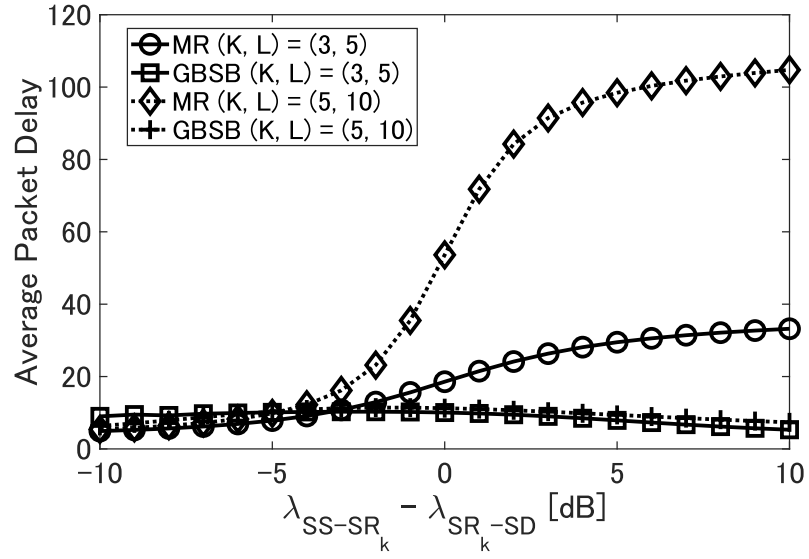


Figure 5.9: Average packet delay of the max-ratio scheme [13] and the proposed scheme, where $\lambda_{\mathrm{SR}_k\text{-SD}}$ was maintained to be $\lambda_{\mathrm{SR}_k\text{-SD}} = 20$ dB.

$\lambda_{\text{SS-SR}_k} < \lambda_{\text{SR}_k\text{-SD}}$, respectively, hence suffering from the detrimental effects of empty and full buffer states. By contrast, the proposed scheme is designed for avoiding these effect, owing to the priority-based relay selection.

Next, Fig. 5.9 shows the average packet delay of the max-ratio and the proposed schemes. As shown in Fig. 5.9, the advantage of the proposed scheme over the max-ratio scheme was seen, especially for $\lambda_{\text{SS-SR}_k} \geq \lambda_{\text{SR}_k\text{-SD}}$. However, in the range of $\lambda_{\text{SS-SR}_k} - \lambda_{\text{SR}_k\text{-SD}} \leq -5$ dB, the packet-delay performance of the max-ratio scheme was nearly the same as that of the proposed scheme.

## 5.5 Summary

In this chapter, the numerical analyses of the max-ratio scheme and the proposed scheme are presented. The effects of $\xi_{\text{SS-SR}}$ and $\xi_{\text{SR-SD}}$ in the proposed scheme are analyzed, where the guidance of designing these two parameters is provided. Numerical results revealed that the proposed scheme outperformed the max-ratio scheme in terms of the outage and packet-delay performance. Besides, the effects of asymmetric channels are discussed, in which the proposed scheme still achieved better outage and packet-delay performance than the conventional max-ratio scheme in most cases.

# Chapter 6

# Conclusions and Future Work

In this thesis, we proposed a novel relay selection scheme in the buffer-aided CRN, which allows us to successfully relax both the effects of inter-network interference and channel fading, by introducing a flexible link selection algorithm in the secondary network. More specifically, we introduced the simultaneous activation of multiple links between the SS and SR nodes, as well as that of the BSB link selection into the buffer-aided cooperative CRN. We also derived the analytical bounds of the outage probability and average packet delay of the proposed scheme. Besides, diversity order and required overheads were investigated. Our numerical results revealed that the proposed scheme is capable of achieving better outage and packet-delay performance than the conventional max-ratio-based scheme. Moreover, since we herein assume that the SD node acts as the central coordinator to process CSI and buffer states information, the distributed manner or other suboptimal alternatives that can reduce the CSI and buffer states information is an open issue left for future studies. Besides, the interference cancellation and physical layer security in the context of the cooperative CRN are also worthy of research.

# References


[1] Claude Elwood Shannon. A mathematical theory of communication. Bell system technical journal, 27(3):379–423, 1948.

[2] Andrew Sendonaris, Elza Erkip, and Behnaam Aazhang. User cooperation diversity–part i: system description. IEEE transactions on communications, 51(11):1927–1938, 2003.

[3] J Nicholas Laneman, David NC Tse, and Gregory W Wornell. Cooperative diversity in wireless networks: Efficient protocols and outage behavior. IEEE Transactions on Information theory, 50(12):3062–3080, 2004.

[4] Andrea Goldsmith. Wireless communications. Cambridge university press, 2005.

[5] Salama S Ikki and Mohamed H Ahmed. Performance analysis of cooperative diversity with incremental-best-relay technique over rayleigh fading channels. IEEE Transactions on Communications, 59(8):2152–2161, 2011.

[6] Edward C Van Der Meulen. Three-terminal communication channels. Advances in applied Probability, 3(1):120–154, 1971.

[7] Nikola Zlatanov, Aissa Ikhlef, Toufiqul Islam, and Robert Schober. Buffer-aided cooperative communications: opportunities and challenges. IEEE Communications Magazine, 52(4):146–153, 2014.

[8] Taneli Riihonen, Stefan Werner, and Risto Wichman. Comparison of full-duplex and half-duplex modes with a fixed amplify-and-forward relay. In 2009 IEEE Wireless Communications and Networking Conference, pages 1–5. IEEE, 2009.

[9] Xiaoyuan Liu, Yanling Zhang, Yang Li, Zhongshan Zhang, and Keping Long. A survey of cognitive radio technologies and their optimization approaches. In 2013 8th International Conference on Communications and Networking in China (CHINACOM), pages 973–978. IEEE, 2013.

[10] Joseph Mitola, Gerald Q Maguire, et al. Cognitive radio: making software radios more personal. IEEE personal communications, 6(4):13–18, 1999.

[11] Ian F Akyildiz, Won-Yeol Lee, Mehmet C Vuran, and Shantidev Mohanty. A survey on spectrum management in cognitive radio networks. 2008.

[12] Manal El Tanab and Walaa Hamouda. Resource allocation for underlay cognitive radio networks: A survey. IEEE Communications Surveys & Tutorials, 19(2):1249–1276, 2016.

[13] Gaojie Chen, Zhao Tian, Yu Gong, and Jonathon Chambers. Decode-and-forward buffer-aided relay selection in cognitive relay networks. IEEE Transactions on Vehicular Technology, 63(9):4723–4728, 2014.

[14] Aggelos Bletsas, Ashish Khisti, David P Reed, and Andrew Lippman. A simple cooperative diversity method based on network path selection. IEEE journal on Selected Areas in Communications, 24(3):659–672, 2006.

[15] Aissa Ikhlef, Diomidis S Michalopoulos, and Robert Schober. Max-max relay selection for relays with buffers. IEEE Transactions on Wireless Communications, 11(3):1124–1135, 2012.

[16] Aissa Ikhlef, Junsu Kim, and Robert Schober. Mimicking full-duplex relaying using half-duplex relays with buffers. IEEE Transactions on Vehicular Technology, 61(7):3025–3037, 2012.

[17] Ioannis Krikidis, Themistoklis Charalambous, and John S Thompson. Buffer-aided relay selection for cooperative diversity systems without delay constraints. IEEE Transactions on Wireless Communications, 11(5):1957–1967, 2012.

[18] Zhao Tian, Gaojie Chen, Yu Gong, Zhi Chen, and Jonathon A Chambers. Buffer-aided max-link relay selection in amplify-and-forward cooperative networks. IEEE Transactions on Vehicular Technology, 64(2):553–565, 2014.

[19] Gaojie Chen, Zhao Tian, Yu Gong, Zhi Chen, and Jonathon A Chambers. Max-ratio relay selection in secure buffer-aided cooperative wireless networks. IEEE transactions on information forensics and security, 9(4):719–729, 2014.

[20] Sheng Luo and Kah Chan Teh. Buffer state based relay selection for buffer-aided cooperative relaying systems. IEEE Transactions on Wireless Communications, 14(10):5430–5439, 2015.

[21] Miharu Oiwa and Shinya Sugiura. Reduced-packet-delay generalized buffer-aided relaying protocol: Simultaneous activation of multiple source-to-relay links. IEEE Access, 4:3632–3646, 2016.

[22] Miharu Oiwa, Chie Tosa, and Shinya Sugiura. Theoretical analysis of hybrid buffer-aided cooperative protocol based on max-max and max-link relay selections. IEEE Transactions on Vehicular Technology, 65(11):9236–9246, 2016.

[23] Ryota Nakai, Miharu Oiwa, Kyungchun Lee, and Shinya Sugiura. Generalized buffer-state-based relay selection with collaborative beamforming. IEEE Transactions on Vehicular Technology, 67(2):1245–1257, 2018.

[24] Ryota Nakai and Shinya Sugiura. Physical layer security in buffer-state-based max-ratio relay selection exploiting broadcasting with cooperative beamforming and jamming. IEEE Transactions on Information Forensics and Security, 14(2):431–444, 2018.

[25] T. Mishina, M. Oiwa, R. Nakai, and S. Sugiura. Buffer-aided virtual full-duplex cooperative networks exploiting source-to-relay broadcast channels. In IEEE 90th Vehicular Technology Conference, Honolulu, Hawaii, USA, September 2019.

[26] R. Nakai and S. Sugiura. Physical layer security in buffer-state-based max-ratio relay selection exploiting broadcasting with cooperative beamforming and jamming. IEEE Transactions on Information Forensics and Security, 14(2):431–444, February 2019.

[27] Zhao Tian, Yu Gong, Gaojie Chen, and Jonathon A Chambers. Buffer-aided relay selection with reduced packet delay in cooperative networks. IEEE Transactions on Vehicular Technology, 66(3):2567–2575, 2016.

[28] Ali Ahmed Mohamed Siddig and Mohd Fadzli Mohd Salleh. Buffer-aided relay selection for cooperative relay networks with certain information rates and delay bounds. IEEE Transactions on Vehicular Technology, 66(11):10499–10514, 2017.

[29] Nikolaos Nomikos, Dimitrios Poulimeneas, Themistoklis Charalambous, Ioannis Krikidis, Demosthenes Vouyioukas, and Mikael Johansson. Delay-and diversity-aware buffer-aided relay selection policies in cooperative networks. IEEE Access, 6:73531–73547, 2018.

[30] Mostafa Darabi, Vahid Jamali, Behrouz Maham, and Robert Schober. Adaptive link selection for cognitive buffer-aided relay networks. IEEE Communications Letters, 19(4):693–696, 2015.

[31] Dingjie Xu, Yichen Gao, Chenchen Yang, Yao Yao, and Bin Xia. Performance analysis of opportunistic cooperation schemes in cognitive radio networks. IEEE Transactions on Vehicular Technology, 67(4):3658–3662, 2017.

[32] Nikola Zlatanov, Robert Schober, and Petar Popovski. Buffer-aided relaying with adaptive link selection. IEEE Journal on Selected Areas in Communications, 31(8):1530–1542, 2013.

[33] Bhupendra Kumar and Shankar Prakriya. Performance of adaptive link selection with buffer-aided relays in underlay cognitive networks. IEEE Transactions on Vehicular Technology, 67(2):1492–1509, 2018.

[34] Jemin Lee, Hano Wang, Jeffrey G Andrews, and Daesik Hong. Outage probability of cognitive relay networks with interference constraints. IEEE Transactions on Wireless Communications, 10(2):390–395, 2011.

[35] Trung Q Duong, Phee Lep Yeoh, Vo Nguyen Quoc Bao, Maged Elkashlan, and Nan Yang. Cognitive relay networks with multiple primary transceivers under spectrum-sharing. IEEE Signal Processing Letters, 19(11):741–744, 2012.

[36] Amos Gilat and V. Subramaniam. Numerical methods for engineers and scientists: An introduction with applications using matlab. 01 2011.

[37] Fumiyuki Adachi, Amnart Boonkajay, Yuta Seki, and Tomoyuki Saito. Mimo channel estimation for time-division duplex distributed antenna cooperative transmission. In 2017 13th International Wireless Communications and Mobile Computing Conference (IWCMC), pages 212–217. IEEE, 2017.

[38] Zhi Yan, Xing Zhang, and Wenbo Wang. Exact outage performance of cognitive relay networks with maximum transmit power limits. IEEE Communications Letters, 15(12):1317–1319, 2011.

[39] Jun-Pyo Hong, Bi Hong, Tae Won Ban, and Wan Choi. On the cooperative diversity gain in underlay cognitive radio systems. IEEE Transactions on Communications, 60(1):209–219, 2011.

[40] Zhao Tian, Gaojie Chen, Yu Gong, Zhi Chen, and Jonathon A Chambers. Buffer-aided max-link relay selection in amplify-and-forward cooperative networks. IEEE Transactions on Vehicular Technology, 64(2):553–565, 2014.

# List of Published Papers

**Journal Articles**

1. Ruichao Zhang, Ryota Nakai, Kaoru Sezaki and Shinya Sugiura. Generalized Buffer-State-Based Relay Selection in Cooperative Cognitive Radio Networks. IEEE Access, 8: 11644-11657, 2020.

**Domestic Conference Papers**

1. Ruichao Zhang, Ryota Nakai, Kaoru Sezaki, and Shinya Sugiura, Buffer-State-Based Relay Selection in Cognitive Radio Networks. IEICE General Conference, March, 2020. (to appear)